Principles of Nonlinear Optical Spectroscopy: A Practical Approach

or: *Mukamel for Dummies*

Peter Hamm

University of Zurich

August 26, 2005

Contents

1 Density Operator

1.1 Density Operator of a Pure State

The density matrix of a pure quantum state $|\psi\rangle$ is defined as:

$$\rho \equiv |\psi\rangle \langle\psi| \tag{1.1}$$

When expanding ψ in a basis $|n\rangle$, we get for the ket

$$|\psi\rangle = \sum_n c_n |n\rangle \tag{1.2}$$

and for the bra, i.e. the Hermitian conjugate

$$\langle\psi| = \sum_n c_n^* \langle n| \tag{1.3}$$

$$\Rightarrow \quad \rho = \sum_{n,m} c_n c_m^* |n\rangle \langle m| \tag{1.4}$$

and the matrix elements of the density operator are:

$$\rho_{nm} \equiv \langle n| \rho |m\rangle = c_n c_m^* \tag{1.5}$$

The expectation value of an operator A is defined as:

$$\langle A\rangle \equiv \langle\psi| A |\psi\rangle \tag{1.6}$$

or, when expanding in the basis $|n\rangle$:

$$\langle A\rangle = \sum_{nm} c_n c_m^* A_{mn} \tag{1.7}$$

$$\Rightarrow \quad \langle A\rangle = \sum_{nm} \rho_{nm} A_{mn} \tag{1.8}$$

$$\langle A\rangle = \mathrm{Tr}\,(A\rho) \tag{1.9}$$

The trace of a matrix B is defined as:

$$\mathrm{Tr}\,(B) \equiv \sum_n B_{nn} \tag{1.10}$$

Properties of the trace:

- The trace is invariant to cyclic permutation: $Tr\,(ABC) = Tr\,(CAB) = Tr\,(BCA)$
- from which follows that the trace of a commutator vanishes: $\mathrm{Tr}\,([A,B]) = \mathrm{Tr}\,(AB - BA) = \mathrm{Tr}\,(AB) - \mathrm{Tr}\,(BA) = 0$
- The trace is invariant to unitary transformation (i.e. is invariant to the basis): $\mathrm{Tr}\,(Q^{-1}AQ) = \mathrm{Tr}\,(QQ^{-1}A) = \mathrm{Tr}\,(A)$

1.2 Time Evolution of the Density Operator

The time evolution of the density matrix:

$$\frac{d}{dt}\rho = \frac{d}{dt}\left(|\psi\rangle\langle\psi|\right) = \left(\frac{d}{dt}|\psi\rangle\right)\cdot\langle\psi| + |\psi\rangle\cdot\left(\frac{d}{dt}\langle\psi|\right) \tag{1.11}$$

The Schrödinger equation describes the time evolution of $|\psi\rangle$:

$$\frac{d}{dt}|\psi\rangle = -\frac{i}{\hbar}H|\psi\rangle \tag{1.12}$$

and for $\langle\psi|$:

$$\frac{d}{dt}\langle\psi| = +\frac{i}{\hbar}\langle\psi|H \tag{1.13}$$

$$\Rightarrow \quad \frac{d}{dt}\rho = -\frac{i}{\hbar}H|\psi\rangle\langle\psi| + \frac{i}{\hbar}|\psi\rangle\langle\psi|H \tag{1.14}$$

$$\frac{d}{dt}\rho = -\frac{i}{\hbar}H\rho + \frac{i}{\hbar}\rho H \tag{1.15}$$

$$\frac{d}{dt}\rho = -\frac{i}{\hbar}[H,\rho] \tag{1.16}$$

This is the *Liouville-Von Neumann* equation

1.3 Density Operator of a Statistical Average

So far, we have discussed the density matrix of a pure state $\rho = |\psi\rangle \langle\psi|$. We just have re-written the equations, but haven't add any new physics (yet!). We can just as well use the wavefunction directly. For example, both equations

$$\frac{d}{dt}|\psi\rangle = -\frac{i}{\hbar}H|\psi\rangle \quad \Leftrightarrow \quad \frac{d}{dt}\rho = -\frac{i}{\hbar}[H,\rho] \tag{1.17}$$

are identical, as long as ρ is the density matrix of a pure state!

However, in condensed phase systems, we in general have to deal with statistical ensembles, rather than pure states. There is no way to write a wavefunction of a statistical average, but we can write the density matrix of a statistical average. Let P_k be the probability of a system being in a pure state $|\psi_k\rangle$, then the density matrix is defined as:

$$\rho = \sum_k P_k \cdot |\psi_k\rangle \langle\psi_k| \tag{1.18}$$

with $P_k \geq 0$

and $\sum_k P_k = 1$ (normalization)

Note (!) that this is by no means equivalent to a wavefunction of the form

$$\theta \stackrel{?}{=} \sum_k P_k \cdot |\psi_k\rangle \tag{1.19}$$

which would be still a pure state (however, not normalized)

Properties of the density matrix:

- The density matrix is Hermitian: $\rho_{nm} = \rho^*_{mn}$
- The diagonal elements of ρ are non-negative: $\rho_{nn} \geq 0$

$\Rightarrow$ ρ_{nn} can be viewed as the probability of the system to be found in state $|n\rangle$

- $\mathrm{Tr}(\rho) = 1$ (normalization)
- $\mathrm{Tr}(\rho^2) \leq 1$ (in general)
- $\mathrm{Tr}(\rho^2) = 1$ (only for a pure state)

Since Equ. 1.9 and Equ. 1.16 are linear in ρ, we still have for the expectation value of an operator A:

$$\langle A \rangle = \mathrm{Tr}\,(A\rho) \tag{1.20}$$

and for the time evolution of the density matrix:

$$\frac{d}{dt}\rho = -\frac{i}{\hbar}\,[H, \rho] \tag{1.21}$$

Example:

Let $|\psi\rangle$ be one of the basis states of a two-level system

$$|\psi\rangle = |1\rangle \rightarrow \rho = \begin{pmatrix} 1 & 0 \\ 0 & 0 \end{pmatrix} \tag{1.22}$$

or

$$|\psi\rangle = |2\rangle \rightarrow \rho = \begin{pmatrix} 0 & 0 \\ 0 & 1 \end{pmatrix} \tag{1.23}$$

For a coherent superposition state of both, which is still a pure state

$$\begin{aligned} &|\psi\rangle = {}^{1}\!/\!_{\sqrt{2}}\,(|1\rangle + |2\rangle) \\ &\Rightarrow \rho_{nm} = c_n c_m^* = \begin{pmatrix} 1/2 & 1/2 \\ 1/2 & 1/2 \end{pmatrix} \end{aligned} \tag{1.24}$$

On the other hand, for a statistical average of both states with $P_1 = P_2$=0.5 we obtain:

$$\rho = \begin{pmatrix} 1/2 & 0 \\ 0 & 1/2 \end{pmatrix} \tag{1.25}$$

As the diagonal elements are the same, the probability of finding the system in either $|1\rangle$ or $|2\rangle$ will be 0.5 in both cases, regardless whether the state is a coherent superposition state (Equ. 1.24) or a statistical average (Equ. 1.25). However, both states are not identical, as seen from the off-diagonal elements which describe the coherence between both states.

Note (!) that there is no wavefunction $|\psi\rangle$ which would give

$$\rho \stackrel{?}{=} |\psi\rangle\,\langle\psi| = \begin{pmatrix} 1/2 & 0 \\ 0 & 1/2 \end{pmatrix} \tag{1.26}$$

1.4 Time Evolution of the Density Matrix of a Two-Level System: No Perturbation

The time evolution of the density matrix

$$\frac{d}{dt}\rho = -\frac{i}{\hbar}\left[H, \rho\right] \tag{1.27}$$

in the eigenstate basis of H:

$$H = \begin{pmatrix} \varepsilon_1 & 0 \\ 0 & \varepsilon_2 \end{pmatrix} \tag{1.28}$$

is

$$\begin{aligned} \frac{d}{dt}\begin{pmatrix} \rho_{11} & \rho_{12} \\ \rho_{21} & \rho_{22} \end{pmatrix} &= -\frac{i}{\hbar}\left[\begin{pmatrix} \varepsilon_1 & 0 \\ 0 & \varepsilon_2 \end{pmatrix}\begin{pmatrix} \rho_{11} & \rho_{12} \\ \rho_{21} & \rho_{22} \end{pmatrix} - \begin{pmatrix} \rho_{11} & \rho_{12} \\ \rho_{21} & \rho_{22} \end{pmatrix}\begin{pmatrix} \varepsilon_1 & 0 \\ 0 & \varepsilon_2 \end{pmatrix}\right] \\ &= -\frac{i}{\hbar}\begin{pmatrix} 0 & (\varepsilon_1 - \varepsilon_2)\rho_{12} \\ (\varepsilon_2 - \varepsilon_1)\rho_{21} & 0 \end{pmatrix} \end{aligned} \tag{1.29}$$

or

$$\begin{aligned} \dot{\rho}_{11} = 0 \quad &\Rightarrow \rho_{11}(t) = \rho_{11}(0) \\ \dot{\rho}_{22} = 0 \quad &\Rightarrow \rho_{22}(t) = \rho_{22}(0) \end{aligned} \tag{1.30}$$

and

$$\begin{aligned} \dot{\rho}_{12} = -\frac{i}{\hbar}\left(\varepsilon_1 - \varepsilon_2\right)\rho_{12} \quad &\Rightarrow \rho_{12}(t) = e^{-i\frac{(\varepsilon_1-\varepsilon_2)}{\hbar}t}\rho_{12}(0) \\ \dot{\rho}_{21} = -\frac{i}{\hbar}\left(\varepsilon_2 - \varepsilon_1\right)\rho_{21} \quad &\Rightarrow \rho_{21}(t) = e^{+i\frac{(\varepsilon_1-\varepsilon_2)}{\hbar}t}\rho_{21}(0) \end{aligned} \tag{1.31}$$

The diagonal elements are stationary in time, and the off-diagonal elements oscillate with the frequency splitting$(\varepsilon_1 - \varepsilon_2)/\hbar$.

1.5 Density Operator in Liouville Representation

We can re-write Equ. 1.29 in the form:

$$\frac{d}{dt}\begin{pmatrix} \rho_{12} \\ \rho_{21} \\ \rho_{11} \\ \rho_{22} \end{pmatrix} = -\frac{i}{\hbar}\begin{bmatrix} \varepsilon_1 - \varepsilon_2 & & & \\ & \varepsilon_2 - \varepsilon_1 & & \\ & & 0 & \\ & & & 0 \end{bmatrix} \cdot \begin{pmatrix} \rho_{12} \\ \rho_{21} \\ \rho_{11} \\ \rho_{22} \end{pmatrix} \tag{1.32}$$

which is the *Liouville representation*. In Liouville space, the operator ρ is written as a vector, and the operation $[H, ...]$ as a superoperator L.

$$\frac{d}{dt}\rho = -\frac{i}{\hbar}L\rho \tag{1.33}$$

or, expanded in a basis:

$$\frac{d}{dt}\rho_{nm} = -\frac{i}{\hbar}\sum_{kl} L_{mn,kl}\rho_{kl} \tag{1.34}$$

This is the *Liouville Equation*. L is a matrix with 4 indexes, which connects each element of ρ (which by itself is a matrix with 2 indexes) with each element. However, note that Equ. 1.33 is just a way of re-writing the Liouville-von Neumann equation Equ. 1.16, but does not yet contain any new physics. As we will see in the next paragraph, it will contain new physics when we include dephasing. Note that the Liouville equation Equ. 1.33 is formally equivalent to the Schrödinger equation.

$$\frac{d}{dt}|\psi\rangle = -\frac{i}{\hbar}H|\psi\rangle \tag{1.35}$$

1.6 Dephasing

The simplest approach to describe dephasing phenomenologically is:

$$\begin{aligned}\dot{\rho}_{12} &= -\frac{i}{\hbar}(\varepsilon_1 - \varepsilon_2)\rho_{12} - \Gamma\rho_{12} \\ \dot{\rho}_{21} &= -\frac{i}{\hbar}(\varepsilon_2 - \varepsilon_1)\rho_{21} - \Gamma\rho_{21}\end{aligned} \tag{1.36}$$

which yields:

$$\rho_{12}(t) = e^{-i\frac{(\varepsilon_1-\varepsilon_2)}{\hbar}t}e^{-\Gamma t}\rho_{12}(0) \tag{1.37}$$

$$\rho_{21}(t) = e^{+i\frac{(\varepsilon_1-\varepsilon_2)}{\hbar}t}e^{-\Gamma t}\rho_{21}(0) \tag{1.38}$$

There is no way to describe dephasing in the wavefunction picture. Equ. 1.36 is by no means equivalent to an expression of the form

$$\frac{d}{dt}|\psi\rangle \stackrel{?}{=} -\frac{i}{\hbar}H|\psi\rangle - \Gamma|\psi\rangle \tag{1.39}$$

which is physically not very meaningful (e.g. $|\psi\rangle$ will not stay normalized)!

Even though dephasing can be described using the density matrix (i.e. Equ. 1.36), the much more compact and elegant way uses the Liouville representation:

$$\frac{d}{dt}\rho = -\frac{i}{\hbar}L\rho - \Gamma\rho \tag{1.40}$$

or, when expanding in a basis:

$$\frac{d}{dt}\rho_{nm} = -\frac{i}{\hbar}\sum_{kl} L_{nm,kl}\rho_{kl} - \sum_{kl}\Gamma_{nm,kl}\rho_{kl} \tag{1.41}$$

Again, L and Γ are matrices with 4 indeces, which connect each element of ρ (which by itself is a matrix with 2 indexes) with each element. There is no such compact matrix representation in the density matrix picture; it can only be done for each matrix element ρ_{ij} of the density operator separately (i.e. Equ. 1.36).

1.7 Hierarchy of Representations

To summarize Sec. 1.1 to 1.6, we have introduced a hierarchy of 3 representations:

(i) The Schrödinger equation acting on wavefunctions:

$$\frac{d}{dt}|\psi\rangle = -\frac{i}{\hbar}H|\psi\rangle \tag{1.42}$$

(ii) The Liouville von Neumann equation acting on the density matrix:

$$\frac{d}{dt}\rho = -\frac{i}{\hbar}[H,\rho] \tag{1.43}$$

(iii) The Liouville equation acting on the density matrix using superoperators

$$\frac{d}{dt}\rho = -\frac{i}{\hbar}L\rho \tag{1.44}$$

From each level of this hierarchy to the next, we have in a first step just re-written the former without adding any new physics. However, each level allows to add new physics (we don't necessarily have to do, but we will). For example, the physics of a density matrix of a pure state is the same as using the wavefunction directly. However, introducing the density matrix allows describing statistical averages, which is impossible in the wavefunction picture. The same is true for the step to the Liouville representation, which allows a much more compact description of dephasing.

1.8 Time Evolution of the Density Matrix of a Two-Level System: Optical Bloch Equation

Let the Hamiltonian be the system Hamiltonian H_0 plus an interaction with an optical light field:

$$H = H_0 - E(t) \cdot \mu \tag{1.45}$$

with

$$E(t) \equiv 2E_0 \cos(\omega t) = E_0 \left(e^{i\omega t} + e^{-i\omega t}\right) \tag{1.46}$$

which in the eigenstate basis of H_0 is:

$$H = \varepsilon_1 |1\rangle \langle 1| + \varepsilon_2 |2\rangle \langle 2| - \mu \cdot E(t) \left(|1\rangle \langle 2| + |2\rangle \langle 1|\right) \tag{1.47}$$

or

$$H = \begin{pmatrix} \varepsilon_1 & -\mu E(t) \\ -\mu E(t) & \varepsilon_2 \end{pmatrix} \tag{1.48}$$

Here, μ is the so-called transition dipole operator, which in the presence of an external electric field $E(t)$ connects the two states $|1\rangle$ and $|2\rangle$. The Liouville von Neumann equation

$$\frac{d}{dt}\rho = -\frac{i}{\hbar}[H, \rho] \tag{1.49}$$

reads in Liouville space:

$$\frac{d}{dt}\begin{pmatrix} \rho_{12} \\ \rho_{21} \\ \rho_{11} \\ \rho_{22} \end{pmatrix} = -\frac{i}{\hbar}\begin{bmatrix} \varepsilon_1 - \varepsilon_2 & 0 & -\mu E(t) & \mu E(t) \\ 0 & \varepsilon_2 - \varepsilon_1 & \mu E(t) & -\mu E(t) \\ -\mu E(t) & \mu E(t) & 0 & 0 \\ \mu E(t) & -\mu E(t) & 0 & 0 \end{bmatrix} \cdot \begin{pmatrix} \rho_{12} \\ \rho_{21} \\ \rho_{11} \\ \rho_{22} \end{pmatrix} \tag{1.50}$$

This is the so-called optical Bloch Equation. In the field free case, we have seen that (see. Equ. 1.31)

$$\rho_{12}(t) = e^{-i\frac{(\varepsilon_1 - \varepsilon_2)}{\hbar}t}\rho_{12}(0) \tag{1.51}$$

$$\rho_{21}(t) = e^{+i\frac{(\varepsilon_1 - \varepsilon_2)}{\hbar}t}\rho_{21}(0) \tag{1.52}$$

Therefore, it is useful to transform into the *rotating frame*:

$$\tilde{\rho}_{12}(t) = e^{-i\omega t}\rho_{12}(t) \tag{1.53}$$

$$\tilde{\rho}_{21}(t) = e^{+i\omega t}\rho_{21}(t) \tag{1.54}$$

and for the diagonal elements:

$$\tilde{\rho}_{11}(t) = \rho_{11}(t) \tag{1.55}$$

$$\tilde{\rho}_{22}(t) = \rho_{22}(t) \tag{1.56}$$

ω is the carrier frequency of the electric field, which will be near resonance $\omega \approx \varepsilon_1 - \varepsilon_2$. In that way, we are separating off the oscillating part $\exp(-i\omega t)$ and keep only the slowly varying envelope $\tilde{\rho}(t)$. When transforming Equ. 1.50 into the rotating frame we obtain:

$$\frac{d}{dt}\begin{pmatrix} \tilde{\rho}_{12} \\ \tilde{\rho}_{21} \\ \tilde{\rho}_{11} \\ \tilde{\rho}_{22} \end{pmatrix} = -i \begin{bmatrix} \Delta & 0 & -\tilde{\Omega}^*(t) & \tilde{\Omega}^*(t) \\ 0 & -\Delta & \tilde{\Omega}(t) & -\tilde{\Omega}(t) \\ -\tilde{\Omega}^*(t) & \tilde{\Omega}(t) & 0 & 0 \\ \tilde{\Omega}^*(t) & -\tilde{\Omega}(t) & 0 & 0 \end{bmatrix} \cdot \begin{pmatrix} \tilde{\rho}_{12} \\ \tilde{\rho}_{21} \\ \tilde{\rho}_{11} \\ \tilde{\rho}_{22} \end{pmatrix} \tag{1.57}$$

with $\Delta = (\varepsilon_1 - \varepsilon_2)/\hbar + \omega$

$$\tilde{\Omega}(t) = \Omega \cdot \left(1 + e^{i2\omega t}\right) = \Omega \cdot \left(e^{-i\omega t} + e^{i\omega t}\right) e^{i\omega t} \tag{1.58}$$

and the Rabi frequency

$$\Omega = \frac{\mu \cdot E_0}{\hbar} \tag{1.59}$$

All frequencies are shifted by $+\omega$ when transforming into the rotating frame. Hence, in the rotating frame, there is a term Ω constant in time and a term oscillating at twice the frequency $\Omega \cdot e^{i2\omega t}$. In other words: As we can separate the real electric field $2E_0 \cos(\omega t)$ into two terms $E_0 (e^{i\omega t} + e^{-i\omega t})$ with positive and negative frequency, we will have one term which rotates in the same direction as the rotating frame, while the second one rotates in opposite direction. When integrating Equ. 1.57, the quickly oscillating term $\Omega \cdot e^{i2\omega t}$ will have essentially no effect. This is since an integral of the

form $\int dt \cdot e^{i2\omega t} f(t)$ will be negligibly small, when $f(t)$ is slowly varying in time; slower than $e^{i2\omega t}$.

Hence, we can replace $\tilde{\Omega}(t) = \Omega$, and the Hamiltonian in Equ. 1.57 is time-independent. This is the *rotating wave approximation* (RWA), which is valid when the electric field is weak enough that the Rabi frequency Ω is slower than the carrier frequency ω. In the RWA, the problem reduces to that of constant coupling:

$$\frac{d}{dt}\tilde{\rho} = -\frac{i}{\hbar}\left[H_{eff}, \tilde{\rho}\right] \tag{1.60}$$

with $H_{eff} = \begin{pmatrix} \hbar\Delta & \hbar\Omega \\ \hbar\Omega & 0 \end{pmatrix}$

In the following figures, the most important situations are discussed. For resonant pumping (Δ=0), we observe Rabi-oscillations with frequency Ω for the diagonal elements of the density matrix ρ_{11} and ρ_{22} (for the initial condition $\rho_{11}(0) = 1$ and $\rho_{22}(0) = 0$):

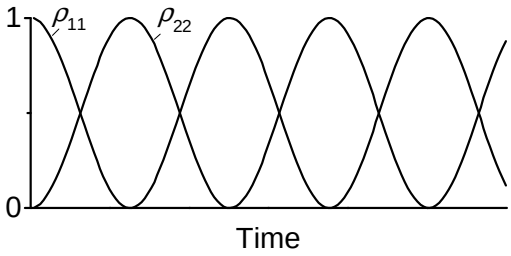

which are less pronounced when the pump field is non-resonant ($\Delta \neq$0):

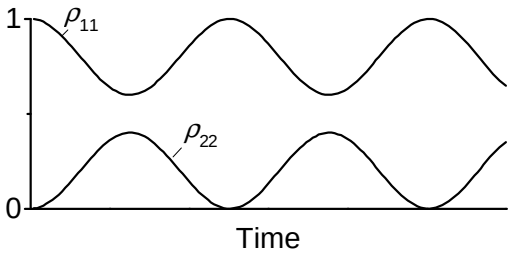

When we add dephasing ($\Gamma << \Omega$p):

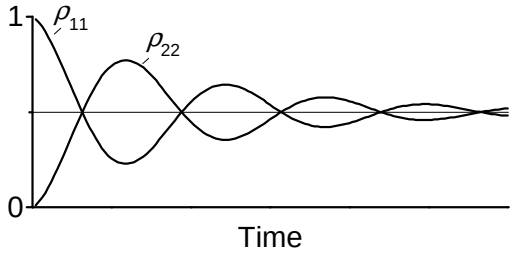

The system looses coherence, i.e. the off-diagonal elements $\tilde{\rho}_{12}(t)$ and $\tilde{\rho}_{21}(t)$ die out and the diagonal elements $\rho_{11}(t)$ and $\rho_{22}(t)$ trend to 1/2. In the case of strong dephasing ($\Gamma >> \Omega$p):

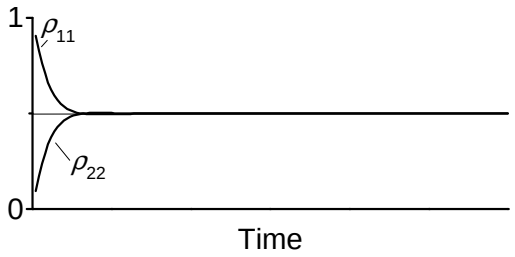

the Bloch oscillations disappear. This is the most common situation in condensed phase systems. For example, the statement found in laser text books: 'One cannot generate an inversion in a 2-level system by optical pumping' is true in the strong-dephasing limit. However, when pumping strong enough that the Rabi oscillation is faster than dephasing, one can in fact generate an inversion in a two level system. In NMR, this is commonly done with π-pulses.

Remark: The Bloch equations have originally been formulated for the case of a classical spin-vector:

$$\frac{d}{dt}\vec{M} = -\gamma \vec{B} \times \vec{M} \tag{1.61}$$

One can show that this equation is equivalent to the optical Bloch equation 1.50 with:

$$\begin{aligned} M_z &= \rho_{11} - \rho_{22} \\ M_x &= \rho_{21} + \rho_{12} \\ M_y &= \rho_{21} - \rho_{12} \end{aligned} \tag{1.62}$$

This connection is very useful since the spin-vector moves in space in a rather intuitive way (like a spinning top).

2 Perturbative Expansion

2.1 Motivation: Non-Perturbative Expansion

We can formally integrate the Schrödinger equation:

$$\frac{d}{dt}\left|\psi(t)\right\rangle = -\frac{i}{\hbar}H(t)\left|\psi(t)\right\rangle \tag{2.1}$$

with the Hamiltonian $H(t)$ being the sum of the system Hamiltonian H_0 and the electric field of a light pulse $E(t)\cdot\mu$ interacting with the system:

$$H(t) = H_0 + E(t)\cdot\mu \tag{2.2}$$

This yields:

$$\left|\psi(t)\right\rangle = \left|\psi(t_0)\right\rangle - \frac{i}{\hbar}\int_{t_0}^{t} d\tau H(\tau)\left|\psi(\tau)\right\rangle \tag{2.3}$$

We can solve this equation iteratively by plugging it into itself:

$$\left|\psi(t)\right\rangle = \left|\psi(t_0)\right\rangle - \frac{i}{\hbar}\int_{t_0}^{t} d\tau H(\tau)\left|\psi(t_0)\right\rangle + \left(-\frac{i}{\hbar}\right)^2\int_{t_0}^{t} d\tau_2\int_{t_0}^{\tau_2} d\tau_1 H(\tau_2)H(\tau_1)\left|\psi(\tau_1)\right\rangle \tag{2.4}$$

and so on:

$$\begin{aligned}\left|\psi(t)\right\rangle \;=\; & \left|\psi(t_0)\right\rangle + \sum_{n=1}^{\infty}\left(-\frac{i}{\hbar}\right)^n\int_{t_0}^{t} d\tau_n\int_{t_0}^{\tau_n} d\tau_{n-1}\ldots\int_{t_0}^{\tau_2} d\tau_1 \\ & H(\tau_n)H(\tau_{n-1})\ldots H(\tau_1)\left|\psi(t_0)\right\rangle\end{aligned} \tag{2.5}$$

Likewise, we can expand the density matrix, the time evolution of which is described by:

$$\frac{d}{dt}\rho = -\frac{i}{\hbar}\left[H,\rho\right] \tag{2.6}$$

which yields:

$$\begin{aligned}\rho(t) = \rho(t_0) + \sum_{n=1}^{\infty}\left(-\frac{i}{\hbar}\right)^n\int_{t_0}^{t} d\tau_n\int_{t_0}^{\tau_n} d\tau_{n-1}\ldots\int_{t_0}^{\tau_2} d\tau_1 \\ \left[H(\tau_n),\left[H(\tau_{n-1}),\ldots\left[H(\tau_1),\rho(t_0)\right]\ldots\right]\right]\end{aligned} \tag{2.7}$$

This expression looks very similar to our final expression Equ. 2.37. However, it is not very useful since it would not converge (not at all, or extremely slowly). The reason is, we did not make use of any knowledge we in general have about the system. It is a non-perturbative expansion. In general, the interaction with the electric field $E(t) \cdot \mu$ will be much weaker than the internal fields of the molecule, and hence, can be treated perturbatively assuming we know the stationary states of the molecule itself (even though in general the quantum mechanics of the molecule itself is extremely complicated, we often just pretend that we know it by writing down eigenstates $|i\rangle$ with eigenenergies ε_i). To get to a perturbative expansion, we have to introduce the concepts of (i) the time evolution operator and the (ii) interaction picture.

2.2 Time Evolution Operator

Let the Hamiltonian H be time-independent. Then, the time evolution operator $U(t,t_0)$ is defined as:

$$|\psi(t)\rangle \equiv U(t,t_0)\,|\psi(t_0)\rangle \tag{2.8}$$

Propagating a wavepacket in an eigenstate basis $|n\rangle$ yields:

$$|\psi(t)\rangle = \sum_n e^{-i\frac{\varepsilon_n}{\hbar}(t-t_0)}\,|n\rangle\,\langle n \mid \psi(t_0)\rangle \tag{2.9}$$

$$\Rightarrow \quad U(t,t_0) = \sum_n e^{-i\frac{\varepsilon_n}{\hbar}(t-t_0)}\,|n\rangle\,\langle n| \tag{2.10}$$

or, in a basis free representation:

$$U_0(t,t_0) = e^{-\frac{i}{\hbar}H\cdot(t-t_0)} \tag{2.11}$$

where the exponential function of an operator A is defined by its Taylor expansion:

$$e^A \equiv 1 + A + \frac{A^2}{2} + \frac{A^3}{6} + ... = 1 + \sum_{n=1}^{\infty}\frac{A^n}{n!} \tag{2.12}$$

Note that Equ. 2.11 is only valid for a time-independent Hamiltonian H.

When introducing the definition of the time evolution operator into the Schrödinger equation, we obtain for its time derivative:

$$\begin{aligned} \frac{d}{dt}\,|\psi(t)\rangle &= -\frac{i}{\hbar}H\,|\psi(t)\rangle \\ \frac{d}{dt}U(t,t_0)\,|\psi(t_0)\rangle &= -\frac{i}{\hbar}H\cdot U(t,t_0)\,|\psi(t_0)\rangle \end{aligned} \tag{2.13}$$

Since this must be valid for any wavefunction $|\psi(t_0)\rangle$, we get

$$\frac{d}{dt}U(t,t_0) = -\frac{i}{\hbar}H \cdot U(t,t_0) \tag{2.14}$$

Properties of the Time Evolution Operator:

- $U(t_0,t_0) = 1$
- $U(t_2,t_0) = U(t_2,t_1)U(t_1,t_0)$
- U is unitary: $U^\dagger(t,t_0)U(t,t_0) = 1$ since $U^\dagger(t,t_0) = U(t_0,t)$
- $U(t,t_0)$ depends only on the time interval $t-t_0$ and is often replaced by $G(t-t_0)$

2.3 Interaction Picture

Let the Hamiltonian now be time-dependent, however, assuming that the time-dependent part is weak and can be treated perturbatively:

$$H(t) = H_0 + H'(t) \tag{2.15}$$

The time evolution operator with respect to the system Hamiltonian H_0 is:

$$U_0(t,t_0) = e^{-\frac{i}{\hbar}H_0\cdot(t-t_0)} \tag{2.16}$$

We define the wavefunction in the interaction picture:

$$|\psi(t)\rangle \equiv U_0(t,t_0)\,|\psi_I(t)\rangle \tag{2.17}$$

In the following, the subscript I denotes interaction picture. $|\psi(t)\rangle$ is the wavefunction under subject of the full Hamiltonian $H(t)$, whereas $U_0(t,t_0)$ is the time evolution operator with respect to the system Hamiltonian H_0 only. Hence, the time dependence of $|\psi_I(t)\rangle$ describes the time evolution of the wavefunction caused by the difference between $H(t)$ and H_0, i.e the weak perturbation $H'(t)$. If that difference is zero, $|\psi_I(t)\rangle$ will be constant in time:

$$|\psi_I(t)\rangle = |\psi(t_0)\rangle \tag{2.18}$$

When introducing Equ. 2.17 into the Schrödinger equation:

$$\begin{aligned} -\frac{i}{\hbar}H\left|\psi(t)\right\rangle &= \frac{d}{dt}\left|\psi(t)\right\rangle \qquad (2.19)\\ -\frac{i}{\hbar}H(t)\cdot U_0(t,t_0)\left|\psi_I(t)\right\rangle &= \frac{d}{dt}\left(U_0(t,t_0)\left|\psi_I(t)\right\rangle\right)\\ &= \left(\frac{d}{dt}U_0(t,t_0)\right)\cdot\left|\psi_I(t)\right\rangle + U_0(t,t_0)\left(\frac{d}{dt}\left|\psi_I(t)\right\rangle\right)\\ &= -\frac{i}{\hbar}H_0\cdot U_0(t,t_0)\cdot\left|\psi_I(t)\right\rangle + U_0(t,t_0)\cdot\left(\frac{d}{dt}\left|\psi_I(t)\right\rangle\right) \end{aligned}$$

since $H'(t) = H(t) - H_0$ we get:

$$-\frac{i}{\hbar}H'(t)\cdot U_0(t,t_0)\left|\psi_I(t)\right\rangle = U_0(t,t_0)\cdot\left(\frac{d}{dt}\left|\psi_I(t)\right\rangle\right) \qquad (2.20)$$

or

$$-\frac{i}{\hbar}U_0^\dagger(t,t_0)H'(t)\cdot U_0(t,t_0)\left|\psi_I(t)\right\rangle = \frac{d}{dt}\left|\psi_I(t)\right\rangle \qquad (2.21)$$

$$\Rightarrow \quad \frac{d}{dt}\left|\psi_I(t)\right\rangle = -\frac{i}{\hbar}H_I'(t)\left|\psi_I(t)\right\rangle \qquad (2.22)$$

where the weak perturbation H_I' in the interaction picture is defined as:

$$H_I'(t) = U_0^\dagger(t,t_0)H'(t)U_0(t,t_0) \qquad (2.23)$$

or

$$H_I'(t) = e^{\frac{i}{\hbar}H_0\cdot(t-t_0)}H'(t)e^{-\frac{i}{\hbar}H_0\cdot(t-t_0)} \qquad (2.24)$$

2.4 Remark: Heisenberg Picture

The interaction picture is a representation between the Schrödinger picture and the Heisenberg picture. The interaction picture adopts the Schrödinger picture for the small perturbation H', while it uses the Heisenberg picture for the larger system Hamiltonian H_0.

In the Schrödinger picture, wavefunctions are time-dependent and follow the time-dependent Schrödinger equation:

$$\begin{aligned} \frac{d}{dt}\psi(t) &= -\frac{i}{\hbar}H\psi(t) \\ \Rightarrow \Psi(t) &= e^{-\frac{i}{\hbar}H\cdot(t-t_0)}\Psi(t_0) \end{aligned} \tag{2.25}$$

Operators, which are used to describe experimental observables, are time independent. The time-dependence of an experimental observation is given by the expectation value of the corresponding (time-independent) operator A:

$$\langle A\rangle(t) = \langle\Psi(t)|A|\Psi(t)\rangle \tag{2.26}$$

where the time-dependence enters through the time-dependent wavefunction.

In the Heisenberg picture, in contrast, operators are time-dependent, and follow the equation:

$$\frac{d}{dt}A_h(t) = -\frac{i}{\hbar}[H, A_H(t)] \tag{2.27}$$

with

$$A_H(t) = e^{\frac{i}{\hbar}H\cdot(t-t_0)}Ae^{-\frac{i}{\hbar}H\cdot(t-t_0)} \tag{2.28}$$

One can show that the Heisenberg wavefunction is just the normal wavefunction at t_0, $\Psi_H = \Psi(t_0)$, and hence, is time-independent. Of course, both pictures are identical, and just a matter of the point of view. In particular, we get for the outcome of an experiment:

$$\langle\Psi(t)|A|\Psi(t)\rangle = \langle\Psi_H|A_H(t)|\Psi_H\rangle \tag{2.29}$$

2.5 Perturbative Expansion of the Wavefunction

Equ. 2.22 is formally equivalent to the Schrödinger equation Equ. 2.1, and can be solved iteratively along the same lines as in Sec. 2.1:

$$\begin{aligned} |\psi_I(t)\rangle = |\psi_I(t_0)\rangle \quad + \quad \sum_{n=1}^{\infty}\left(-\frac{i}{\hbar}\right)^n \int_{t_0}^{t} d\tau_n \int_{t_0}^{\tau_n} d\tau_{n-1}\ldots\int_{t_0}^{\tau_2} d\tau_1 \\ H_I'(\tau_n)H_I'(\tau_{n-1})\ldots H_I'(\tau_1)\,|\psi_I(t_0)\rangle \end{aligned} \tag{2.30}$$

The important difference now is that this is an expansion in powers of the weak perturbation $H'(t)$, and not the full Hamiltonian $H(t)$. Going back to the Schrödinger picture, we obtain when using $|\psi(t)\rangle \equiv U_0(t,t_0)\,|\psi_I(t)\rangle$ and $|\psi(t_0)\rangle = |\psi_I(t_0)\rangle$:

$$|\psi(t)\rangle = \left|\psi^{(0)}(t)\right\rangle + \sum_{n=1}^{\infty}\left(-\frac{i}{\hbar}\right)^n \int_{t_0}^{t} d\tau_n \int_{t_0}^{\tau_n} d\tau_{n-1} \ldots \int_{t_0}^{\tau_2} d\tau_1 \tag{2.31}$$
$$U_0(t,t_0)H'_I(\tau_n)H'_I(\tau_{n-1})\ldots H'_I(\tau_1)\,|\psi(t_0)\rangle$$

where $\left|\psi^{(0)}(t)\right\rangle \equiv U_0(t,t_0)\,|\psi(t_0)\rangle$ is the zero-order wavefunction, i.e. the wavefunction without subject to the perturbation $H'(t)$. When writing the interaction Hamiltonian in the Schrödinger picture using $H'_I(t) = U_0^{\dagger}(t,t_0)H'(t)U_0(t,t_0)$, we obtain:

$$|\psi(t)\rangle = |\psi(t_0)\rangle + \sum_{n=1}^{\infty}\left(-\frac{i}{\hbar}\right)^n \int_{t_0}^{t} d\tau_n \int_{t_0}^{\tau_n} d\tau_{n-1} \ldots \int_{t_0}^{\tau_2} d\tau_1 \tag{2.32}$$
$$U_0(t,\tau_n)H'(\tau_n)U_0(\tau_n,\tau_{n-1})H'(\tau_{n-1})\ldots U_0(\tau_2,\tau_1)H'(\tau_1)U_0(\tau_1,t_0)\,|\psi(t_0)\rangle$$

where we have used $U(\tau_n,\tau_{n-1}) = U(\tau_n,t_0)U(t_0,\tau_{n-1}) = U(\tau_n,t_0)U^{\dagger}(\tau_{n-1},t_0)$. This expression has an intuitive physical interpretation: The system propagates under subject of the system Hamiltonian H_0 (i.e. propagates *freely*) until time τ_1, described by the time evolution operator $U(\tau_1,t_0)$. At time τ_1, it interacts with the perturbation $H'(\tau_1)$. Subsequently, it again propagates freely until time τ_2, and so on. This interpretation leads directly to the graphic representation of Feynman diagrams:

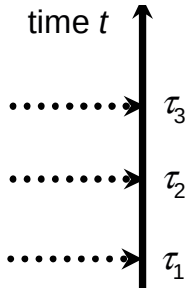

where the vertical arrow depicts the time axis, and the dotted arrows depict interaction with the perturbation H' at the time points $\tau_{1,}$, τ_2 and so on. The perturbative expansion of a wavefunction is represented by a *single sided* Feynman diagram.

2.6 Perturbative Expansion of the Density Matrix

Along the same lines, we can develop a power expansion of the density matrix. To this end, we first define the density matrix in the interaction picture:

$$|\psi(t)\rangle\,\langle\psi(t)| = U_0(t,t_0)\cdot|\psi_I(t)\rangle\,\langle\psi_I(t)|\cdot U_0^{\dagger}(t,t_0) \tag{2.33}$$

or

$$\rho(t) = U_0(t, t_0) \cdot \rho_I(t) \cdot U_0^\dagger(t, t_0) \tag{2.34}$$

Since this expression is linear in ρ, it also holds for a statistical average $\rho = \sum_k P_k \left|\psi\right\rangle \left\langle\psi\right|$. Since the time evolution of the wavefunction in the interaction picture $|\psi_I(t)\rangle$ is formally equivalent to the Schrödinger equation (see Equ. 2.22), the same is true for the density matrix in the interaction picture, for which we obtain an equation which is formally equivalent to the Liouville von Neumann equation

$$\frac{d}{dt}\rho_I(t) = -\frac{i}{\hbar}\left[H_I'(t), \rho_I(t)\right] \tag{2.35}$$

Its power expansion is (see Equ. 2.7)

$$\begin{aligned} \rho_I(t) &= \rho_I(t_0) + \sum_{n=1}^{\infty}\left(-\frac{i}{\hbar}\right)^n \int_{t_0}^{t} d\tau_n \int_{t_0}^{\tau_n} d\tau_{n-1} \ldots \int_{t_0}^{\tau_2} d\tau_1 \\ &\quad [H_I'(\tau_n), [H_I'(\tau_{n-1}), \ldots [H_I'(\tau_1), \rho_I(t_0)] \ldots]] \end{aligned} \tag{2.36}$$

Going back to the Schrödinger picture yields:

$$\begin{aligned} \rho(t) &= \rho^{(0)}(t) + \sum_{n=1}^{\infty}\left(-\frac{i}{\hbar}\right)^n \int_{t_0}^{t} d\tau_n \int_{t_0}^{\tau_n} d\tau_{n-1} \ldots \int_{t_0}^{\tau_2} d\tau_1 \\ &\quad U_0(t, t_0) \cdot [H_I'(\tau_n), [H_I'(\tau_{n-1}), \ldots [H_I'(\tau_1), \rho(t_0)] \ldots]] \cdot U_0^\dagger(t, t_0) \end{aligned} \tag{2.37}$$

The interaction Hamiltonian is still in the interaction picture and contains both the perturbation H'(t) and time evolution operators, similar to Equ. 2.32. However, since the density matrix contains a ket and a bra, the interaction can be either from the left or the right. We will see this in Sec. 3.1 when writing the commutators explicitly.

When we assume that $\rho(\mathrm{t_0})$ is an equilibrium density matrix it does not evolve in time under subject of the system Hamiltonian H_0, and we can send $t_0 \to -\infty$. Furthermore, we now specify the perturbation

$$H'(t) = E(t) \cdot \mu \tag{2.38}$$

and get:

$$\rho(t) = \rho^{(0)}(-\infty) + \sum_{n=1}^{\infty} \rho^{(n)}(t) \tag{2.39}$$

with the n^{th}-order density matrix given by

$$\rho^{(n)}(t) = \left(-\frac{i}{\hbar}\right)^n \int_{-\infty}^{t} d\tau_n \int_{-\infty}^{\tau_n} d\tau_{n-1} \ldots \int_{-\infty}^{\tau_2} d\tau_1 E(\tau_n)E(\tau_{n-1}) \cdot \ldots \cdot E(\tau_1) \cdot \quad (2.40)$$
$$U_0(t,t_0) \cdot [\mu_I(\tau_n), [\mu_I(\tau_{n-1}), \ldots [\mu_I(\tau_1), \rho(-\infty)] \ldots]] \cdot U_0^\dagger(t,t_0)$$

Here, the dipole operator in the interaction picture is defined as:

$$\mu_I(t) = U_0^\dagger(t,t_0)\mu U_0(t,t_0) \quad (2.41)$$

In the Schrödinger picture, the dipole operator μ is time-independent. It is time-dependent in the interaction picture since the system is evolving in time under subject of the system Hamiltonian H_0. The subscript I (which denotes interaction picture) is commonly discarded, and Schrödinger picture versus interaction picture is specified implicitly by writing either μ or $\mu(t)$, respectively.

2.7 Short Excursion into Nonlinear Optics

The electric displacement is

$$D = \varepsilon_0 E + P \quad (2.42)$$

where E is the incident electric field and P the macroscopic polarization as a response to it. In linear optics, the polarization depends linearly on the electric field E:

$$P = \varepsilon_0 \chi^{(1)} \cdot E \quad (2.43)$$

with $\chi^{(1)}$ the linear susceptibility. However, for high enough electric fields this is no longer true. Therefore, we expand the polarization in powers of the electric field E:

$$P = \varepsilon_0 \left(\chi^{(1)} \cdot E + \chi^{(2)} \cdot E \cdot E + \chi^{(3)} \cdot E \cdot E \cdot E + \ldots\right) \quad (2.44)$$

with the nonlinear susceptibilities $\chi^{(n)}$. Taking into account that the electric field is in fact a vector, the linear and nonlinear susceptibilities become tensors. In media with inversion symmetry, such as isotropic media, even-order susceptibilities vanish. This is since the polarization must change its sign when the optical electric fields are reversed. Therefore, for most media the lowest order nonlinearity is the 3^{rd}-order nonlinearity.

The macroscopic polarization is given by the expectation value of the dipole operator μ:

$$P(t) = \mathrm{Tr}(\mu\rho(t)) \equiv \langle \mu\rho(t) \rangle \tag{2.45}$$

where $\langle \ldots \rangle$ is the expectation value Equ. 1.9). For example, we get for a two level system:

$$\mu = \begin{pmatrix} 0 & \mu_{12} \\ \mu_{21} & 0 \end{pmatrix} \tag{2.46}$$

and

$$\langle \mu\rho(t) \rangle = \left\langle \begin{pmatrix} 0 & \mu_{12} \\ \mu_{21} & 0 \end{pmatrix} \begin{pmatrix} \rho_{11} & \rho_{12} \\ \rho_{21} & \rho_{22} \end{pmatrix} \right\rangle = \rho_{12}\mu_{21} + \rho_{21}\mu_{12} \tag{2.47}$$

Hence, off-diagonal elements of the density matrix give rise to a macroscopic polarization and emit a light field.

When now collecting the terms in powers of the electric field $E(t)$ (compare Equ. 2.40 and 2.44), we obtain for the n^{th}-order polarization:

$$P^{(n)}(t) = \left\langle \mu\rho^{(n)}(t) \right\rangle \tag{2.48}$$

2.8 Nonlinear Polarization

When inserting Equ. 2.40 into Equ. 2.48, we obtain for the n^{th} order polarization

$$\begin{aligned} P^{(n)}(t) = & \left(-\frac{i}{\hbar}\right)^n \int_{-\infty}^{t} d\tau_n \int_{-\infty}^{\tau_n} d\tau_{n-1} \ldots \int_{-\infty}^{\tau_2} d\tau_1 E(\tau_n)E(\tau_{n-1}) \cdot \ldots \cdot E(\tau_1) \\ & \langle \mu(t) \cdot [\mu(\tau_n), [\mu(\tau_{n-1}), \ldots [\mu(\tau_1), \rho(-\infty)] \ldots]] \rangle \end{aligned} \tag{2.49}$$

Here, we made use of the definition of the dipole operator in the interaction picture (discarding the subscript I) $\mu(t) = U_0^\dagger(t, t_0)\mu U_0(t, t_0)$ and the invariance of the trace $\langle \ldots \rangle$ to cyclic permutation. Frequently, a different set of time variables is used:

$$\begin{aligned} \tau_1 &= 0 \\ t_1 &= \tau_2 - \tau_1 \\ t_2 &= \tau_3 - \tau_2 \\ &\vdots \\ t_n &= t - \tau_n \end{aligned} \tag{2.50}$$

We can choose $\tau_1 = 0$ since the time-zero point is arbitrary. The time variables $\tau_n$denote absolute time points, while the time variables t_1 denote time intervals:

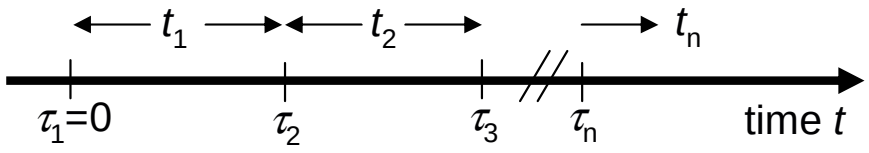

Transforming Equ. 2.49 into this set of time variables gives:

$$\begin{aligned} P^{(n)}(t) &= \left(-\frac{i}{\hbar}\right)^n \int_0^\infty dt_n \int_0^\infty dt_{n-1} \ldots \int_0^\infty dt_1 \\ &\quad E(t-t_n)E(t-t_n-t_{n-1}) \cdot \ldots \cdot E(t-t_n-t_{n-1}-\ldots-t_1) \cdot \\ &\quad \langle \mu(t_n+t_{n-1}+\ldots t_1)\,[\mu(t_{n-1}+\ldots+t_1), \ldots [\mu(0), \rho(-\infty)]\ldots]\rangle \end{aligned} \tag{2.51}$$

Hence, the n^{th}-order nonlinear response can be written as a convolution of n electric fields

$$\begin{aligned} P^{(n)}(t) &= \int_0^\infty dt_n \int_0^\infty dt_{n-1} \ldots \int_0^\infty dt_1 \\ &\quad E(t-t_n)E(t-t_n-t_{n-1}) \cdot \ldots \cdot E(t-t_n-\ldots-t_1) \cdot S(t_n, t_{n-1}, \ldots, t_1) \end{aligned} \tag{2.52}$$

with the n^{th}-order nonlinear response function:

$$S^{(n)}(t_n, \ldots t_1) = \left(-\frac{i}{\hbar}\right)^n \langle \mu(t_n+\ldots t_1)\,[\mu(t_{n-1}+\ldots+t_1), \ldots [\mu(0), \rho(-\infty)]\ldots]\rangle \tag{2.53}$$

The response function is defined for positive times t_n only. Note the different role of the last interaction $\mu(t_n + t_{n-1} + \ldots t_1)$ compared to the previous interactions: The interactions at times 0, t_1, ... and t_{n-1}+...+t_1 generate a non-equilibrium density matrix $\rho^{(n)}$, whose off-diagonal elements at time $t_n + t_{n-1}$+...+t_1 emit a light field. Only the first n interactions are part of the commutators, while the last is not.

3 Double Sided Feynman Diagrams

3.1 Liouville Pathways

When writing the cummutator in Equ. 2.53

$$\langle \mu(t_n + t_{n-1} + \ldots t_1) \left[\mu(t_{n-1} + \ldots + t_1), \ldots \left[\mu(0), \rho(-\infty) \right] \ldots \right] \rangle \tag{3.1}$$

explicitly, we obtain 2^n terms with various numbers of interactions acting either on the left (i.e. on the ket) or the right (i.e. on the bra) of the density matrix. Within these terms there are pairs of terms which are the conjugate complex of each other. Hence, it is sufficient to consider only 2^{n-1} terms. We illustrate this for the most important cases, namely linear and 3^{rd} order response. The linear response function is:

$$\begin{aligned} S^{(1)}(t_1) &= -\frac{i}{\hbar} \langle \mu(t_1) \left[\mu(0), \rho(-\infty) \right] \rangle = \\ & -\frac{i}{\hbar} \left(\langle \mu(t_1)\mu(0)\rho(-\infty) \rangle - \langle \mu(t_1)\rho(-\infty)\mu(0) \rangle \right) = \\ & -\frac{i}{\hbar} \left(\langle \mu(t_1)\mu(0)\rho(-\infty) \rangle - \langle \rho(-\infty)\mu(0)\mu(t_1) \rangle \right) = \\ & -\frac{i}{\hbar} \left(\langle \mu(t_1)\mu(0)\rho(-\infty) \rangle - \langle \mu(t_1)\mu(0)\rho(-\infty) \rangle^* \right) \end{aligned} \tag{3.2}$$

Here, we have made use of the invariance of the trace on cyclic permutation and, in the last step, of:

$$\left\langle \left(\mu(t_1)\mu(0)\rho(-\infty) \right)^\dagger \right\rangle = \left\langle \rho^\dagger(-\infty)\mu^\dagger(0)\mu^\dagger(t_1) \right\rangle = \langle \rho(-\infty)\mu(0)\mu(t_1) \rangle \tag{3.3}$$

since all operators are Hermitian (they are operators of observables).The Feynman diagrams corresponding to both terms are:

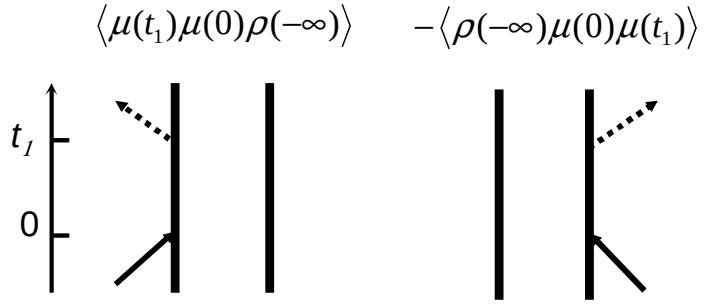

The left vertical line denotes the time evolution of the ket of the density matrix, and the right arrow that of the bra. The interactions with the dipole operator are indicated

by arrows acting either on the ket or the bra (i.e. from the left or the right). The right diagram is the conjugate complex of the left, and therefore is not shown explicitly in general. By convention, we will show only diagrams with the last interaction emitting form the ket (i.e. the left side). Note the different role of the first interaction, which is responsible for the perturbation of the density matrix, while the last one originates from (see Equ. 2.48)

$$P^{(n)}(t) = \left\langle \mu\rho^{(n)}(t) \right\rangle \tag{3.4}$$

and represents emission of light from the non-equilibrium density matrix. This difference is generally indicated by using a different arrow in the Feynman diagrams.

For the 3^{rd} order nonlinear response we get:

$$\begin{aligned}
&\langle \mu(t_3+t_2+t_1)\,[\mu(t_2+t_1),[\mu(t_1),[\mu(0),\rho(-\infty)]]]\rangle = \\
&= \langle \mu(t_3+t_2+t_1)\mu(t_2+t_1)\mu(t_1)\mu(0)\rho(-\infty)\rangle && \Rightarrow R_4 \\
&- \langle \mu(t_3+t_2+t_1)\mu(t_2+t_1)\mu(t_1)\rho(-\infty)\mu(0)\rangle && \Rightarrow R_1^* \\
&- \langle \mu(t_3+t_2+t_1)\mu(t_2+t_1)\mu(0)\rho(-\infty)\mu(t_1)\rangle && \Rightarrow R_2^* \\
&+ \langle \mu(t_3+t_2+t_1)\mu(t_2+t_1)\rho(-\infty)\mu(0)\mu(t_1)\rangle && \Rightarrow R_3 \\
&- \langle \mu(t_3+t_2+t_1)\mu(t_1)\mu(0)\rho(-\infty)\mu(t_2+t_1)\rangle && \Rightarrow R_3^* \\
&+ \langle \mu(t_3+t_2+t_1)\mu(t_1)\rho(-\infty)\mu(0)\mu(t_2+t_1)\rangle && \Rightarrow R_2 \\
&+ \langle \mu(t_3+t_2+t_1)\mu(0)\rho(-\infty)\mu(t_1)\mu(t_2+t_1)\rangle && \Rightarrow R_1 \\
&- \langle \mu(t_3+t_2+t_1)\rho(-\infty)\mu(0)\mu(t_1)\mu(t_2+t_1)\rangle && \Rightarrow R_4^*
\end{aligned} \tag{3.5}$$

Along the same lines as in Equ. 3.2 we see that the terms R_1^*, R_2^*, R_3^* and R_4^* are the conjugate complex of $R_{1,}R_2$, R_3 and R_4. The corresponding Feynman diagrams are:

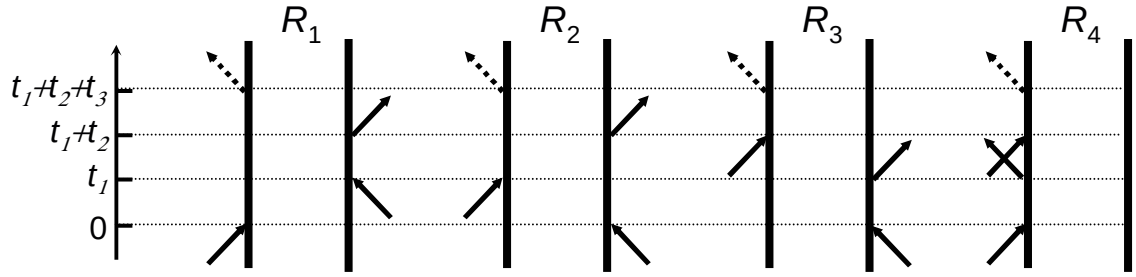

Feynman Diagrams: Rules

1. Vertical lines represent the time evolution of the ket and bra of the density matrix. Time is running from the bottom to the top.

2. Interactions with the light field are represented by arrows. The last interaction, which originates from the trace $P^{(n)}(t) = \left\langle \mu\rho^{(n)}(t) \right\rangle$, is different in character and hence is often indicated using a different arrow.

3. Each diagram has a sign $(-1)^n$, where n is the number of interactions from the right. This is since each time an interaction is from the right in the commutator it carries a minus sign. Since the last interaction is not part of the commutator, it is not counted in this sign-rule.

4. An arrow pointing to the right represents an electric field with $e^{-i\omega t+ikr}$, while an arrow pointing to the left represents an electric field with $e^{+i\omega t-ikr}$. This rule expresses the fact that the real electric field $E(t) = 2E_0(t)\cdot\cos(\omega t - kr)$can be separated into positive and negative frequencies $E(t) = E_0(t)\cdot\left(e^{-i\omega t+ikr} + e^{+i\omega t-ikr}\right)$. The emitted light, i.e. the last interaction, has a frequency and wavevector which is the sum of the input frequencies and wavevectors (considering the appropriate signs).

5. An arrow pointing towards the system represents an up-climbing of the corresponding side of the density matrix, while an arrow pointing away represents a de-excitation. This rule is a consequence of the rotating wave approximation (see below). Since the last interaction corresponds to an emission of light, it always points away from the system.

6. The last interaction must end in a population state.

In addition to the 2^{n-1} terms of the nonlinear response function, the electric field separates into many terms. To illustrate this, we consider the 3^{rd} order response as an example:

$$P^{(3)}(t) = \int_0^\infty dt_3 \int_0^\infty dt_2 \int_0^\infty dt_1 E(t-t_3)E(t-t_3-t_2)E(t-t_3-t_2-t_1)S(t_3,t_2,t_1) \tag{3.6}$$

Let's assume the electric field originates from 3 laser pulses centered at time t=0 and after delay times τ and T:

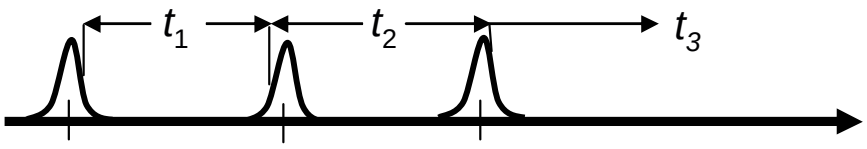

Each electric field which enters Equ. 3.6 is the sum of the electric fields of 3 laser pulses:

$$\begin{aligned} E(t) &= 2E_1(t)\cdot\cos(\omega t) + 2E_2(t)\cdot\cos(\omega t) + 2E_3(t)\cdot\cos(\omega t) = \\ &= E_1(t)\cdot\left(e^{-i\omega t} + e^{+i\omega t}\right) + E_2(t)\cdot\left(e^{-i\omega t} + e^{+i\omega t}\right) + E_3(t)\cdot\left(e^{-i\omega t} + e^{+i\omega t}\right) \end{aligned} \tag{3.7}$$

and contains 6 terms. Hence, the expression in Equ. 3.6

$$E(t-t_3)E(t-t_3-t_2)E(t-t_3-t_2-t_1)\cdot S(t_3,t_2,t_1) \tag{3.8}$$

contains in total 6·6·6·4=864 terms! Fortunately, there are experimental tricks to reduce the number of terms considerably:

- Time ordering
- Rotating Wave Approximation
- Phase Matching

If all these tricks are applied at the same time, one may reduce the number of terms to 2.

3.2 Time Ordering and Semi-Impulsive Limit

When the laser pulses $E_1(t)$, $E_2(t)$ and $E_3(t)$ are shorter than the time separation between them, they do not overlap in time and we say we have strict time ordering. In that case, we know for sure that the first interaction $\mu(0)$ originates from the pulse $E_1(t)$, $\mu(t_1)$ from $E_2(t)$, and so on. This reduces the number of terms from 6·6·6·4 to 2·2·2·4=32.

In non-linear, time-resolved spectroscopy, we often use the semi-impulsive limit. In this limit, the laser pulses are assumed to be short compared with any time scale of the system but long compared to the oscillation period of the light field. Hence, the envelopes of the pulses are approximated by δ-function.

$$\begin{aligned} E_1(t) &= E_1\delta(t)e^{\pm i\omega t\mp kr} \\ E_2(t) &= E_2\delta(t-\tau)e^{\pm i\omega t\mp kr} \\ E_2(t) &= E_2\delta(t-\tau-T)e^{\pm i\omega t\mp kr} \end{aligned} \tag{3.9}$$

while the pulses still carry a carrier frequency and a wavevector, which we will be needed to calculate the frequency and the wavevector of the emitted light (wave matching condition rule 4). In this limit, we obtain for the 3^{rd} order response

$$P^{(3)}(t) = S(t,T,\tau) \tag{3.10}$$

which reduces the computer effort to simulate the nonlinear polarisation considerably.

3.3 Rotating Wave Approximation

When the rotating wave approximation (RWA) can be applied, only terms containing either $e^{-i\omega t}$or $e^{i\omega t}$ will contribute, but not both (see Sec. 1.8). When we have at the same time strict time ordering of the 3 interacting pulses, the rotating wave approximation reduces the number of terms to 1·1·1·4. We shall illustrate the rotating wave approximation for linear response, whose response function

$$\langle \mu(t_1)\mu(0)\rho(-\infty)\rangle \tag{3.11}$$

is constructed in the following way:

- nothing happens until t=0.
- At t=0, we generate a ρ_{10} off-diagonal matrix element of the density matrix. The probability that this happens is proportional to the transition dipole moment μ_{10}.

$$\rho_{10}(0) \propto \mu_{10} \tag{3.12}$$

- We have calculated in Equ. 1.36 how this off-diagonal density matrix element evolves in time:

$$\Rightarrow \quad \rho_{10}(t) \propto \mu_{10} e^{-i\frac{(\varepsilon_1-\varepsilon_0)}{\hbar}t_1} e^{-\Gamma t_1} \tag{3.13}$$

- At time t_1, the off-diagonal matrix element emits a light field which is again proportional to μ_{10} (see Equ. 2.45):

$$S^{(1)}(t_1) \propto \mu_{10}^2 e^{-i\frac{(\varepsilon_1-\varepsilon_0)}{\hbar}t_1} e^{-\Gamma t_1} \tag{3.14}$$

- For the 1^{st} order polarization, we have to calculate:

$$P^{(1)}(t) = -\frac{i}{\hbar}\int_0^\infty dt_1 E(t-t_1) S^{(1)}(t_1) \tag{3.15}$$

Let's assume the electric field

$$E(t) = 2E_0(t)\cos(\omega t) = E_0(t)\cdot\left(e^{-i\omega t} + e^{+i\omega t}\right) \tag{3.16}$$

is resonant with the system:

$$\omega = \frac{\varepsilon_1 - \varepsilon_0}{\hbar} \tag{3.17}$$

Then, we get:

$$\begin{aligned} P^{(1)}(t) = &-\tfrac{i}{\hbar}\mu_{10}^2 e^{-i\omega t} \int_0^\infty dt_1 E_0(t-t_1) e^{-\Gamma t_1} \\ &-\tfrac{i}{\hbar}\mu_{10}^2 e^{+i\omega t} \int_0^\infty dt_1 E_0(t-t_1) e^{-\Gamma t_1} e^{-i2\omega t_1} \end{aligned} \tag{3.18}$$

The integrand in the first term is slowly varying as a function of time t_1, while that of the second is highly oscillating. The second integral therefore is essentially zero and can in general be neglected. This is the rotating wave approximation (RWA), which is valid for near resonance conditions $\omega \approx (\varepsilon_1 - \varepsilon_0)/\hbar$ and when the envelope of the electric field $E_0(t)$ is slowly varying in time (slower than the carrier frequency ω). In other words: In principle, each diagram has two possibilities to interact with the electric field, either with $e^{-i\omega t}$ or $e^{i\omega t}$. We indicate this using direction of the arrows in the Feynman diagram. The two terms in Equ. 3.18 correspond to the following diagrams (rule 4):

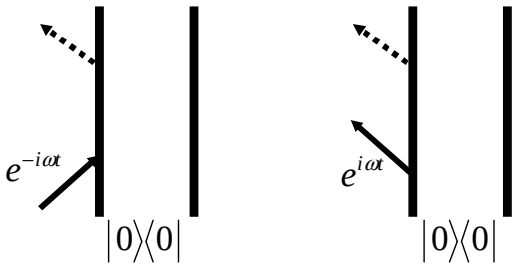

We have seen that the second diagram does not survive the rotating wave approximation. This leads to an intuitive physical interpretation: In the first diagram, the ground state density matrix $|0\rangle\langle 0|$ is excited on the left side (light is going in) to yield $|1\rangle\langle 0|$. The second diagram would correspond to a de-excitation of the ground state, which is of course not possible.

3.4 Phase Matching

When adding wavevectors to the electric fields

$$\begin{aligned} E(t) \;=\; & E_1(t)\left(e^{-i\omega t+ikr} + e^{+i\omega t-ikr}\right) + E_2(t)\left(e^{-i\omega t+ikr} + e^{+i\omega-ikrt}\right) + \\ & E_3(t)\left(e^{-i\omega t+ikr} + e^{+i\omega t-ikr}\right) \end{aligned} \tag{3.19}$$

the product

$$E(t-t_3)E(t-t_3-t_2)E(t-t_3-t_2-t_1) \tag{3.20}$$

will carry a wave vector

$$k = \pm k_1 \pm k_2 \pm k_3 \tag{3.21}$$

However, given the rotating wave approximation is valid, only one set of signs will survive, which allows further reducing of the number of terms. For example, the diagrams:

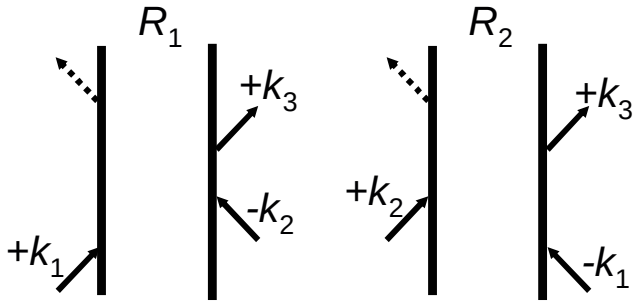

will emit light in different directions, namely R_1 into $k = +k_1 - k_2 + k_3$ and R_2 into $k = -k_1 + k_2 + k_3$. Hence, by designing the geometry of the experimental setup in an intelligent way one can distinguish between different diagrams. This will be discussed extensively in the next paragraph.

4 Nonlinear Spectroscopies

4.1 Linear Spectroscopy

In this chapter, we will discuss various types of non-linear spectroscopies. To start, we first introduce linear spectroscopy. There is only one linear experiment we can perform, namely measuring the (linear) absorption spectrum of a sample. The corresponding Feynman diagram is:

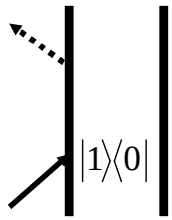

We have already calculated the 1^{st}-order polarization (see Equ. 3.18)

$$P^{(1)}(t) = -\frac{i}{\hbar}\mu_{10}^2 e^{-i\omega_0 t} \int_0^\infty dt_1 E_0(t-t_1) e^{-\Gamma t_1} \tag{4.1}$$

Let's assume $E_0(t)$ is a short pulse and we can apply the semi-impulsive limit:

$$E_0(t) \approx E_0 e^{i\omega t} \cdot \delta(t) \tag{4.2}$$

Then, we get:

$$P^{(1)}(t) = -\frac{i}{\hbar} E_0 \mu_{10}^2 e^{-i\omega_0 t} e^{-\Gamma t} \tag{4.3}$$

The 1^{st}-order polarization emits an electric field with a 90° phase lack:

$$E^{(1)}(t) \propto -iP^{(1)}(t) \tag{4.4}$$

This is the *free induction decay.*

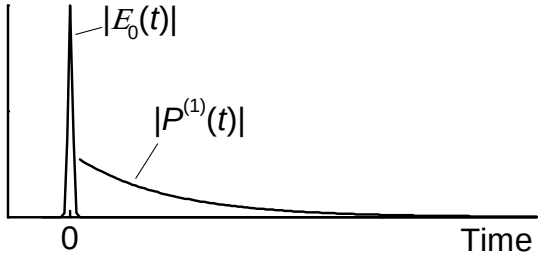

Important for the outcome of an experiment is not just this field, but also the way how this field is detected. The field detection can be controlled by the experimental configuration (i.e. where we put a detectoe). For instance, the most simple form of a absorption measurement measurement would look like this:

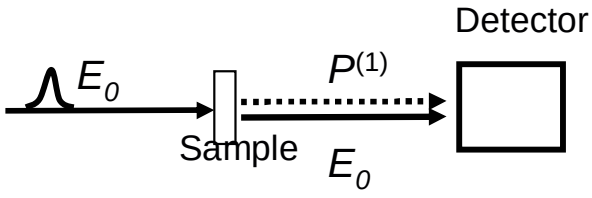

In optical spectroscopy, we typically have so-called square-law detectors, which measure the intensity, rather than the field of the light on the detector. Furthermore, these detectors are slow (compared to the femtosecond timescale), and hence measure the time integrated intensity. Hence, we will measure in such an experiment:

$$\int_0^\infty \left|E_0(t) + E^{(1)}(t)\right|^2 dt = \int_0^\infty |E_0(t)|^2 + \left|E^{(1)}(t)\right|^2 + 2\Re\left(E_0(t)E^{(1)}(t)\right) dt \quad (4.5)$$

In most applications of spectroscopy, however, we will put a spectrometer in front of the detector:

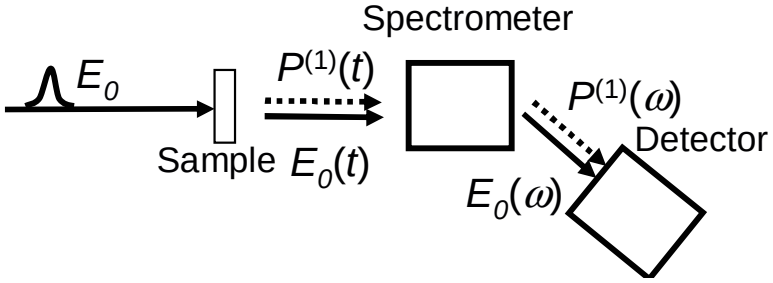

whose action is to perform a Fourier transform of the fields:

$$\left|E_0(\omega) + E^{(1)}(\omega)\right|^2 = |E_0(\omega)|^2 + \left|E^{(1)}(\omega)\right|^2 + 2\Re\left(E_0(\omega)E^{(1)}(\omega)\right) \quad (4.6)$$

Since we discuss a perturbative approach, we can safely assume that the second term is small compared to the others, so that it is in general neglected. In other words, the generated 1^{st} order polarization is *heterodyne* detected, using the input laser pulse itself as a local oscillator.

When we measure an absorption spectrum, we typically normalize the transmitted light with the light in front of the sample:

$$\frac{I}{I_0} \equiv \frac{\left|E_0(\omega) + E^{(1)}(\omega)\right|^2}{\left|E_0(\omega)\right|^2} = 1 + \frac{2\Re\left(E_0(\omega)E^{(1)}(\omega)\right)}{\left|E_0(\omega)\right|^2} \tag{4.7}$$

The absorption spectrum (i.e. the logarithm of this expression), can be written in the small signal case:

$$A(\omega) \propto -\frac{\left|E_0(\omega) + E^{(1)}(\omega)\right|^2}{\left|E_0(\omega)\right|^2} + 1 = -\frac{2\Re\left(E_0(\omega)E^{(1)}(\omega)\right)}{\left|E_0(\omega)\right|^2} = -2\Re\left(E^{(1)}(\omega)\right) \tag{4.8}$$

In the last step, we have used that the laser pulse is a δ-pulse, whose spectrum is constant in frequency. Hence, we get:

$$\begin{aligned} A(\omega) \propto= 2\Im\left(P^{(1)}(\omega)\right) &= 2\Re\int_0^\infty dt \cdot e^{i(\omega-\omega_0)t}e^{-\Gamma t_1} = 2\Re\frac{1}{i\left(\omega-\omega_0\right)-\Gamma} \\ &= \frac{2\Gamma}{\left(\omega-\omega_0\right)^2+\Gamma^2} \end{aligned} \tag{4.9}$$

As expected, the absorption spectrum is a Lorentzian function with a width given by the dephasing rate of the transition.

In general, we find for the absorption spectrum:

$$A(\omega) \propto 2\Re\int_0^\infty dt \cdot e^{i\omega t}\left\langle\mu(t)\mu(0)\rho(-\infty)\right\rangle \tag{4.10}$$

which can be seen when starting directly from Equ. 3.1 (see Sec. 5).

4.2 Pump-Probe Spectroscopy of a 3-Level System

Let's assume a molecule with three states:

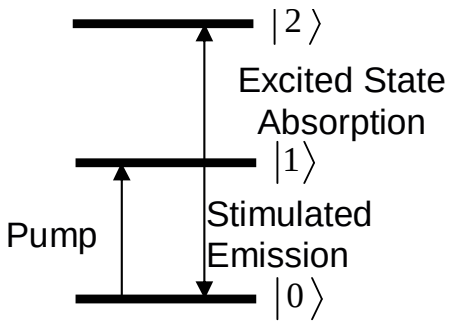

where both the 0→1 and the 1→2 transition are near-resonant with the probe pulse (however, they don't necessarily have exactly the same frequency). In a pump-probe experiment, we use the following geometry:

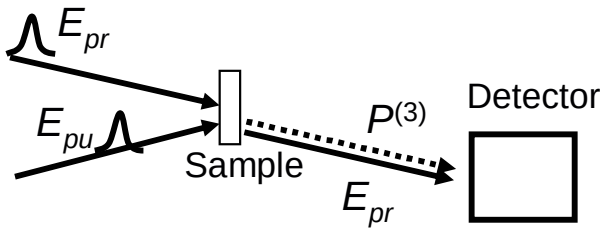

The generated 3^{rd} order polarization is detected in exactly the same direction as the probe pulse itself. As in linear spectroscopy, the generated 3^{rd} order polarization is heterodyne detected using the probe pulse as local oscillator. This geometry has an important consequence for phase matching: The wavevector of the generated 3^{rd} order polarization is the sum of the wavevectors of the generating fields. However, owing to the special geometry chosen in a pump-probe setup, we force the wavevector of the 3^{rd} order polarization to be the same as that of the pump pulse k_{pr}. The only way how this can be achieved is that the pump pulse interacts twice with the sample with wave vectors $+k_{pu}$ and $-k_{pu}$. As a consequence, only 6 diagrams survive the rotating wave approximation and the phase matching condition:

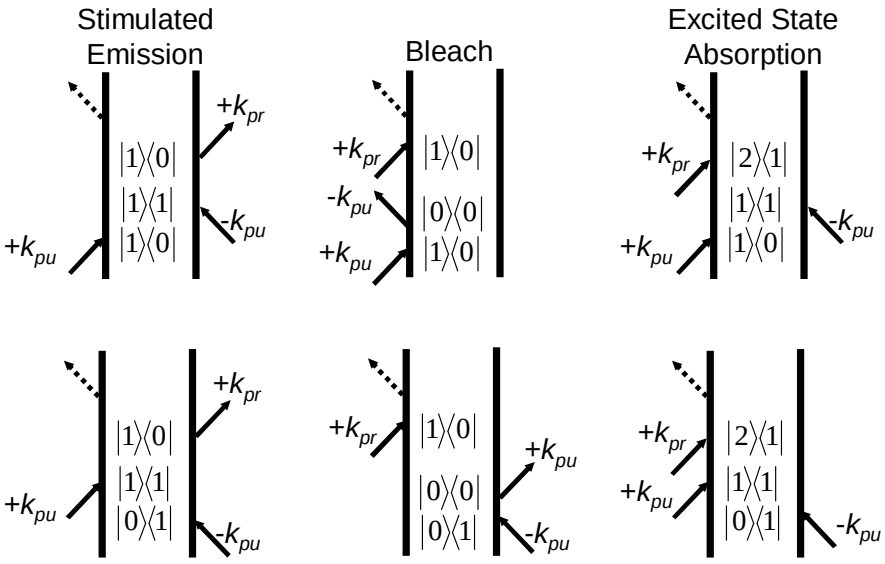

Note that both interactions of the pump pulse come from the same field E_{pu}. Therefore, there is no possibility to select time ordering for the first two interactions. However, we have assumed time ordering between pump and probe pulse, i.e. the probe pulse is the last interaction in all diagrams. When pump and probe pulse overlap in time, additional diagrams would have to be considered. This leads to a phenomenon known as the *coherence spike* or *coherent artifact*.

The left diagrams are pumped to the excited state by the pump pulse and stimulated back to the ground state by the probe pulse. They represent stimulated emission. The middle diagrams describe those molecules which are in the ground state after the pump pulse, and hence represent the bleach contribution. The right diagrams are pumped to the excited state by the pump pulse, from where the second excited state is probed. They represent excited state absorption. Let's first construct the response function for the upper stimulated emission diagram:

- nothing happens until t=0.
- At t=0, we generate a ρ_{10} off-diagonal matrix element of the density matrix with a probability that is proportional to the transition dipole moment μ_{10}:

$$\rho_{10}(0) \propto \mu_{10} \tag{4.11}$$

- This off-diagonal matrix element would now start to oscillate and relax due to dephasing. However, we neglect evolution of the density matrix in the first time period t_1, since we assume that the pump pulse is short (shorter than the dephasing rate), and the second interaction from the left is coming at essentially the same time ($t_1 \approx$0).

- After the second interaction, we have generated a diagonal density matrix ρ_{11} with a probability proportional to $\rho_{11}(0) \propto \mu_{10}^2$
- We have seen in Equ. 1.29. that the diagonal elements of the density matrix stay constant in time (when we neglect population relaxation T_1)

$$\Rightarrow \quad \rho_{11}(t_2) \propto \mu_{10}^2 \tag{4.12}$$

- With the third interaction, a ρ_{10} matrix element is generated, again with probability μ_{10}. The ρ_{10} matrix develops as a function of time t_3:

$$\rho_{10}(t_3) \propto \mu_{10}^3 e^{-i\frac{(\varepsilon_1-\varepsilon_0)}{\hbar}t_3} e^{-\Gamma t_3} \tag{4.13}$$

- After emitting the 3$^{\text{rd}}$-order polarisation with another factor μ_{01} we get for the 3$^{\text{rd}}$-order response function:

$$S_{SE}^{(3)}(t_3, t_2, t_1) \propto \frac{i}{\hbar^3}\mu_{10}^4 e^{-i\frac{(\varepsilon_1-\varepsilon_0)}{\hbar}t_3} e^{-\Gamma t_3} \tag{4.14}$$

The upper-bleach diagram has the same coherences ρ_{10} during the first and the third time period, and hence will be identical to the stimulated emission diagram during these periods. It is different during the second time period t_2, where it is in the ground state ρ_{00} rather than the excited state ρ_{11}. However, since we have assumed in this simple example that nothing is happening during this time, we find that the response function is the same as the stimulated-emission diagram (note that this is not necessarily the case).

$$S_{Bl}^{(3)}(t_3, t_2, t_1) = S_{SE}^{(3)}(t_1, t_2, t_3) \tag{4.15}$$

The upper-excited state absorption diagram is identical with the stimulated emission diagram until the 3^{rd} interaction. After that, a ρ_{21} coherence is generated with probability μ_{21}:

$$\rho^{(3)}(t_3) \propto -\mu_{10}^2\mu_{21} e^{-i\frac{(\varepsilon_2-\varepsilon_1)}{\hbar}t_3} e^{-\Gamma t_3} \tag{4.16}$$

which gives rise to the 3^{rd} order response

$$S_{ESA}^{(3)}(t_3, t_2, t_1) \propto -\frac{i}{\hbar^2}\mu_{10}^2\mu_{21}^2 e^{-i\frac{(\varepsilon_2-\varepsilon_1)}{\hbar}t_3} e^{-\Gamma t_3} \tag{4.17}$$

Note the minus sign, which originates from the fact that this diagram has 1, rather than 2 interactions from the right (rule (3) in Sec. 3.1). We have assumed that the 01 and the 12 dephasing rates are the same.

Finally, the difference between the bottom-diagrams and the top-diagrams is the time-ordering of the first two interactions from the pump-pulse. However, since we have assumed that the pump pulse is shorter than any time scale of the system (the response functions do not depend on t_1), the bottom-diagrams yield the same nonlinear response as the corresponding diagrams at the top. Hence, we get for the total response:

$$\begin{aligned} S^{(3)}(t_3,t_2,t_1) &= \sum_{i=1}^{6} S_i^{(3)}(t_1,t_2,t_3) \propto \\ & \frac{i}{\hbar^3}\left(4\mu_{10}^4 e^{-i\frac{(\varepsilon_1-\varepsilon_0)}{\hbar}t_3} e^{-\Gamma t_3} - 2\mu_{10}^2\mu_{21}^2 e^{-i\frac{(\varepsilon_2-\varepsilon_1)}{\hbar}t_3} e^{-\Gamma t_3}\right) \end{aligned} \tag{4.18}$$

which, in the semi-impulsive limit, equals the 3^{rd} order polarization:

$$P^{(3)}(t;T,\tau) = S^{(3)}(t,T,\tau) \tag{4.19}$$

The detector measures the generated 3^{rd} order polarization as a function of t by heterodyning it with the original probe pulse (similar to the linear response, see Equ. 4.9):

$$-\log\left(\frac{\left|E_{pr}(t)+iP^{(3)}(t)\right|^2}{\left|E_{pr}(t)\right|^2}\right) \approx -\frac{2\Im\left(E_{pr}(t)P^{(3)}(t)\right)}{\left|E_{pr}(t)\right|^2} \tag{4.20}$$

There are two possibilities to measure the signal: either directly, or after transmitting the light through a spectrometer. In the first case, the detector again measures the time-integrated intensity:

$$\Delta A = 2\Im\int_0^\infty dt E_{pr}(t)P^{(3)}(t) \tag{4.21}$$

In this simple example, the pump-probe signal Equ. 4.21 does not depend on the time separation between both pulses, T (we have assumed that nothing happens during time period t_2).

In the second case, the spectrometer performs a Fourier transform of the fields with respect to time t, and we get for the pump-probe-spectrum:

$$\begin{aligned} \Delta A(\omega) \propto -2\Im\left(P^{(3)}(\omega)\right) &= -\frac{8\mu_{10}^4\Gamma}{\left((\varepsilon_1-\varepsilon_0)/\hbar-\omega\right)^2+\Gamma^2} + \\ & \frac{4\mu_{10}^2\mu_{21}^2\Gamma}{\left((\varepsilon_2-\varepsilon_1)/\hbar-\omega\right)^2+\Gamma^2} \end{aligned} \tag{4.22}$$

where we have used that the probe pulse has been assumed to be a δ-pulse, whose frequency spectrum is a constant. Hence, we will observe a negative Lorentzian line at the original frequency of the 0→1 transition (bleach and stimulated emission) and a positive Lorentzian line at the 1→2 transition (excited state absorption).

4.3 Quantum-Beat Spectroscopy

Now let's assume the following three-level system:

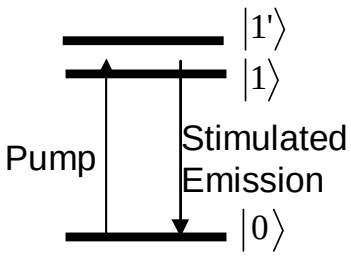

We have put both excited states close together so that both the 0→1 and the 0→1' transition are resonant with the pump pulse. We chose the same pump-probe geometry. In that case, the following Feynman diagrams survive the rotating wave approximation and phase matching condition:

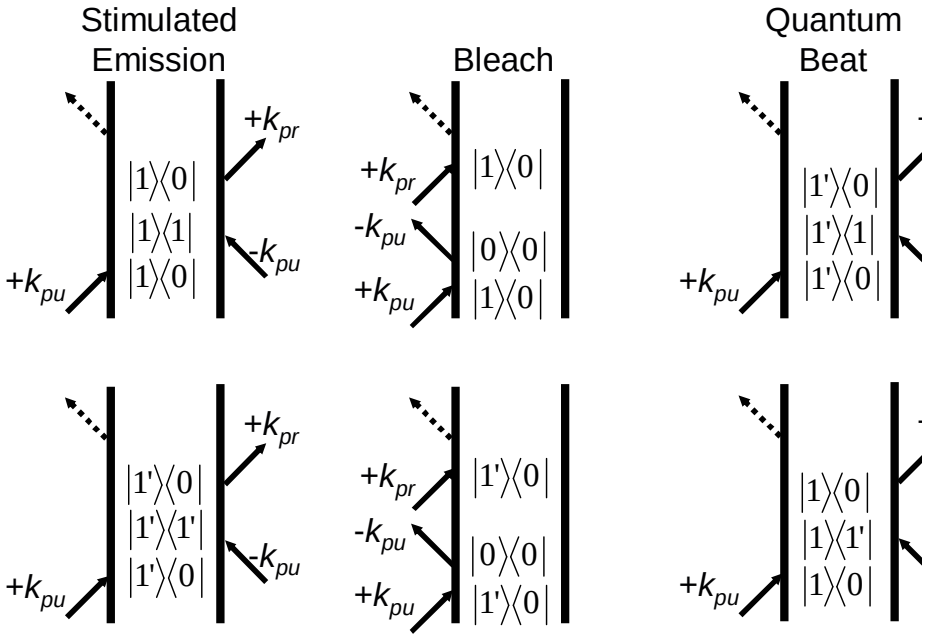

There are additional Feynman diagrams with reversed time ordering of the first two pump pulse interactions. However, we again assume that the pump pulse is short compared to all timescales of the system, and these diagrams will give rise to identical response functions. The stimulated emission and bleach diagrams are the same as before, except that we now have them for 2 resonances 0→1 and 0→1'. The corresponding

response function is:

$$\sum_{i=1}^{4} S_i^{(3)}(t_3,t_2,t_1) \propto -\frac{i}{\hbar^3} 4 \left(\mu_{10}^4 e^{-i\frac{(\varepsilon_1-\varepsilon_0)}{\hbar}t_3} e^{-\Gamma t_3} + \mu_{1'0}^4 e^{-i\frac{\left(\varepsilon_{1'}-\varepsilon_0\right)}{\hbar}t_3} e^{-\Gamma t_3} \right) \tag{4.23}$$

New are the quantum beat diagrams, which oscillate as a function of t_2 with a frequency given by the splitting between both states.

$$\begin{aligned} \sum_{i=5}^{6} S_i^{(3)}(t_3,t_2,t_1) \quad &\propto \quad -\frac{i}{\hbar^3} 2\mu_{10}^2\mu_{1'0}^2 \\ &\left(e^{-i\frac{\left(\varepsilon_{1'}-\varepsilon_1\right)}{\hbar}t_2} e^{-i\frac{\left(\varepsilon_{1'}-\varepsilon_0\right)}{\hbar}t_3} + e^{-i\frac{\left(\varepsilon_1-\varepsilon_{1'}\right)}{\hbar}t_2} e^{-i\frac{(\varepsilon_1-\varepsilon_0)}{\hbar}t_3} \right) e^{-\Gamma t_3} \end{aligned} \tag{4.24}$$

In the semi-impulsive limit we again get:

$$P^{(3)}(t;T,\tau) = \sum_{i=1}^{6} S^{(3)}(t,T,\tau) \tag{4.25}$$

The detector integrates over t:

$$\Delta A(T) = 2\Im \int_0^\infty dt E_{pr}(t) P^{(3)}(t;T) \tag{4.26}$$

The pump-probe signal now depends on the time separation between pump and probe pulse, T. When we scan the delay time we will observe quantum beats with a frequency equal to the spacing between both excited state levels.

4.4 Two-Pulse Photon Echo Spectroscopy

The following geometry is chosen in a two-pulse photon echo experiment:

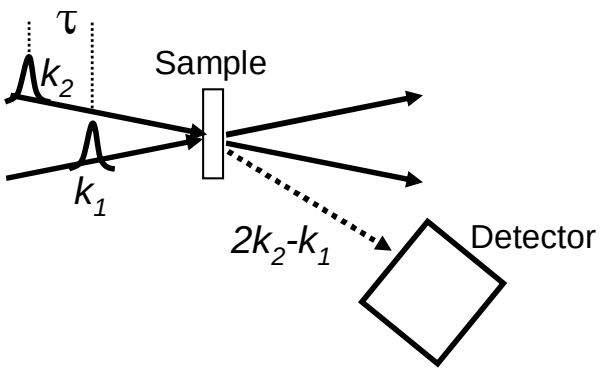

We send two pulses into the sample with wavevectors k_1 and k_2 and the generated 3^{rd} order polarization is detected in the $2k_2$-k_1 direction. This choice of the geometry has two consequences: (i) 2 interactions now come from the second pulse and (ii) the 3^{rd} order polarization is now emitted into a direction which is different from that of the input pulses. Hnece, we will measure the homodyned signal, $\left|P^{(3)}\right|^2$, rather than the heterodyned signal $2\Im\left(E_0 P^{(3)}\right)$. Only two Feynman diagrams survive the rotating wave approximation and phase matching condition (for a 2-level system):

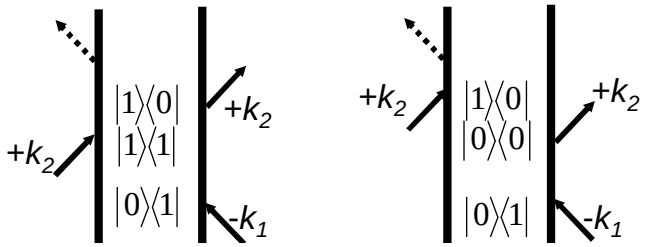

Both diagrams have one feature in common: During the fist time period t_1, they propagate in a ρ_{01} coherence, which is flipped to a ρ_{10} coherence during the last time period t_3. The former is oscillating with $e^{i\omega t}$ while the latter is oscillating in the opposite direction $e^{-i\omega t}$. The flip of the oscillation frequency gives rise to rephasing in very much the same way as known for spin vectors:

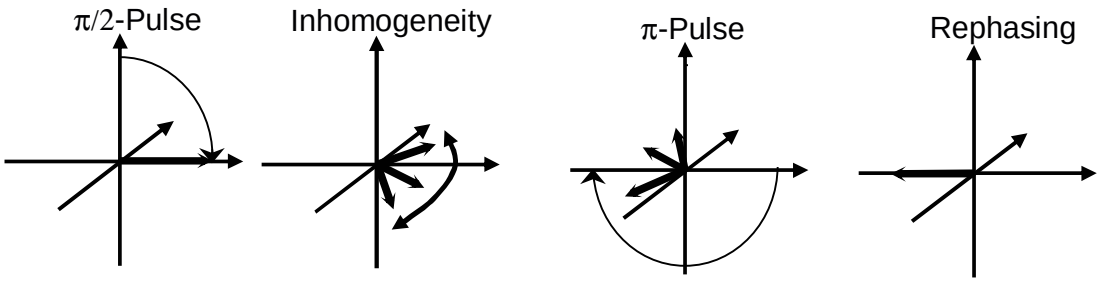

The 1^{st} pulse generates a rotating spin vector. However, in the presence of inhomogeneous broadening, each individual spin will oscillate with a slightly different frequency,

so that the individual spin vectors will spread out and the macroscopic polarization will disappear after some time. The 2^{nd} pulse flips all vectors to the other side, effectively changing the direction of the rotation. As a consequence, all spin vectors will re-combine, a phenomenon called rephasing. They will be recombined perfectly after a time which equals the time separation between both pulses. This is why the phenomenon is called an *echo*.

We shall now see how this picture can be translated to optical spectroscopy. We again assume that the pulses are in the semi-impulsive limit, so that the second and third interactions occur at essentially the same time and we can neglect the 2^{nd} time period t_2. Then both response function are identical:

$$\begin{aligned} S_1^{(3)}(t_3,t_2,t_1) &\propto \frac{i}{\hbar^3}\mu_{10}^4 e^{+i\frac{(\varepsilon_1-\varepsilon_0)}{\hbar}t_1}e^{-\Gamma t_1}e^{-i\frac{(\varepsilon_1-\varepsilon_0)}{\hbar}t_3}e^{-\Gamma t_3} = \\ &= \frac{i}{\hbar^2}\mu_{10}^4 e^{-i\frac{(\varepsilon_1-\varepsilon_0)}{\hbar}(t_3-t_1)}e^{-\Gamma(t_3+t_1)} \end{aligned} \tag{4.27}$$

In the semi-impulsive limit, we get:

$$P^{(3)}(t,\tau) = S^{(3)}(t,0,\tau) \tag{4.28}$$

The detector, which is a slow detector, integrates the emitted intensity over the last time period and hence will measure:

$$\int_0^\infty dt \left|P^{(3)}(t;T,\tau)\right|^2 \propto \frac{\mu_{10}^8}{\hbar^6}e^{-2\Gamma\tau}\cdot\int_0^\infty dt\left|e^{-i\frac{(\varepsilon_1-\varepsilon_0)}{\hbar}t}e^{-\Gamma t}\right|^2 = \frac{\mu_{10}^8}{\hbar^6}e^{-2\Gamma\tau}\cdot const \tag{4.29}$$

Hence, the signal will decay with twice the dephasing rate Γ as a function of time τ. The delay time τ is the time we control in the experiment by varying the time separation between both pulses. Equ. 4.29 is the result for a purely homogeneously broadened line. Inhomogeneous broadening is considered by convoluting the response function with a Gaussian distribution for the energy splitting

$$S_1^{(3)}(t_3,t_2,t_1) \rightarrow \int d\varepsilon_{10} G\left(\varepsilon_{10}-\varepsilon_{10}^{(0)}\right) S_1^{(3)}(t_3,t_2,t_1) \tag{4.30}$$

where $\varepsilon_{10} \equiv \varepsilon_1 - \varepsilon_0$ and $\varepsilon_{10}^{(0)}$ is the center frequency of this distribution. Using the Fourier transform of the distribution function, we obtain:

$$P^{(3)}(t;T,\tau) \propto \frac{i}{\hbar^3}\mu_{10}^4 e^{-i\frac{\varepsilon_{10}^{(0)}}{\hbar}(\tau-t)}e^{-\Gamma(\tau+t)}e^{-\sigma^2\frac{(\tau-t)^2}{2}} \tag{4.31}$$

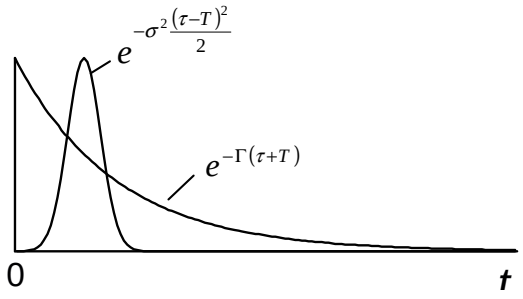

where σ is the width of the inhomogeneous distribution. For a particular setting of delay time τ, the emitted light as a function of t will be a product of two terms: $e^{-\Gamma(\tau+t)}$ and $e^{-\sigma^2\frac{(\tau-t)^2}{2}}$:

The inhomogeneous distribution acts as a gate, and light is emitted predominantly after a time which is equal to the time separation between both pulses τ. The following picture depicts the sequence of pulses:

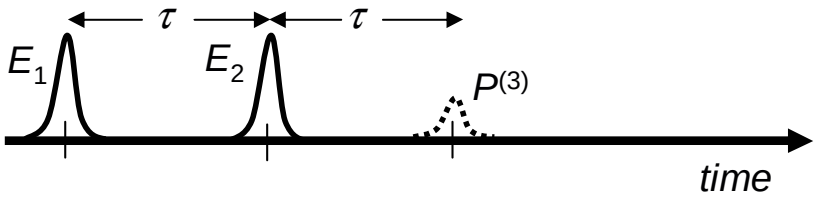

In the limit of infinitely broad inhomogeneous broadening, the Gaussina distribution will converge to a δ-distribution:

$$e^{-\sigma^2\frac{(\tau-t)^2}{2}} \rightarrow \delta(\tau - t) \tag{4.32}$$

and we obtain for the signal:

$$\int_0^\infty dt \left|P^{(3)}(t;T,\tau)\right|^2 \propto \frac{\mu_{10}^8}{\hbar^6} e^{-2\Gamma\tau} \int_0^\infty dt \left|e^{-i\frac{(\varepsilon_1-\varepsilon_0)}{\hbar}t} e^{-\Gamma t}\delta(\tau - t)\right|^2 \propto \frac{\mu_{10}^8}{\hbar^6} e^{-4\Gamma\tau} \tag{4.33}$$

Hence, in the case of large inhomogeneous broadening, the signal decays with 4 times the dephasing rate.

For intermediate situations (finite inhomogeneous broadening), we observe a *peak shift* when we scan the time separation τ between both pulses. This shall be rationalized using the following sequence of pictures:

The detector measures the time integral of the emitted filed (the shaded area), which initially rises as a function of τ. For large enough decay times it will decay with a

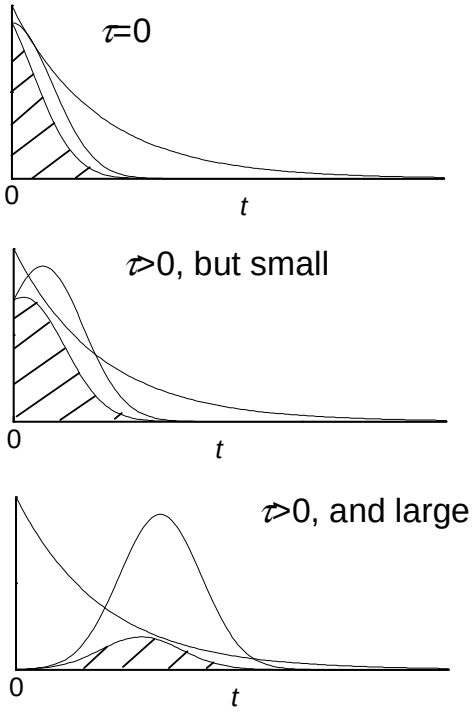

slope which again is 4 times the dephasing rate. Hence, there will be a maximum for a certain delay time $\tau>0$ which is known as the *peak shift* and which is a commonly used as a measure of the strength of inhomogeneous broadening. An example of such an experiment on the asymmetric stretching vibration of N_3^- dissolved in H_2O is shown below:

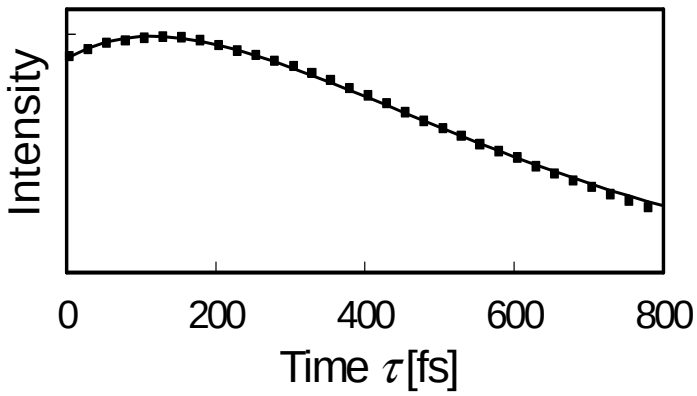

5 Microscopic Theory of Dephasing: Kubo's Stochastic Theory of Line Shapes

5.1 Linear Response

The Feynman diagram describing linear response is:

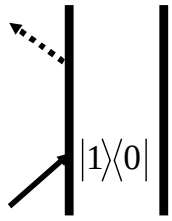

The corresponding response function is:

$$S^{(1)}(t) = -\frac{i}{\hbar}\left\langle \mu(t)\mu(0)\rho(-\infty)\right\rangle \tag{5.1}$$

Let's recall that $\mu(t)$ is the dipole operator in the interaction picture:

$$\mu(t) = e^{+\frac{i}{\hbar}H\cdot t}\mu e^{-\frac{i}{\hbar}H\cdot t} \tag{5.2}$$

When we expand $\mu(t)$ in a eigenstate basis of H we obtain for the $\mu_{01}(t)$ matrix element:

$$\mu_{01}(t) = e^{+\frac{i}{\hbar}\varepsilon_0 t}\cdot\mu_{01}\cdot e^{-\frac{i}{\hbar}\varepsilon_1 t} = e^{-\frac{i}{\hbar}(\varepsilon_1-\varepsilon_0)t}\cdot\mu_{01} \tag{5.3}$$

and likewise for $\mu_{10}(t)$ matrix element:

$$\mu_{10}(t) = e^{+\frac{i}{\hbar}(\varepsilon_1-\varepsilon_0)t}\cdot\mu_{10} \tag{5.4}$$

This result is conform with rule (4) in Sec. 3.1. For example, the right-going arrow in the above picture carries a frequency term $e^{-i\omega t}$, which will cancel with the $e^{+\hbar/(\varepsilon_1-\varepsilon_0)t}$ term of μ_{10} in the resonant case. Hence, we can rewrite Equ. 5.1:

$$S^{(1)}(t) = -\frac{i}{\hbar}\left\langle \mu_{01}(t)\mu_{10}(0)\rho_{00}\right\rangle \tag{5.5}$$

This notation distinguishes between excitation of the ket of the density matrix at time 0, $\mu_{10}(0)$, and de-excitation at time t, $\mu_{01}(t)$. The sign-rules are automatically taken

care of when choosing the indices such that identical levels are next to each other in Equ. 5.5.

At this point, we make a crude approximation, in that we interpret the quantum mechanical operators $\mu_{01}(t)$ as classical observables. Then we get:

$$\mu_{01}(t) = e^{-i\omega t}\mu_{01}(0) \tag{5.6}$$

with

$$\omega \equiv \frac{(\varepsilon_1 - \varepsilon_0)}{\hbar} \tag{5.7}$$

the energy gap frequency. Equ. 5.6 describes, for example, a diatomic molecule in the vacuum. When we kick it, it will start to vibrate with a particular frequency ω. When there is no perturbation (i.e., in vacuum), it would continue to vibrate with that frequency for ever. However, in the presence of a bath, the surrounding will constantly push and pull at the molecule and cause a stochastic force on the molecule. This will give rise to a time-dependent frequency $\omega(t)$. To obtain an expression equivalent to Equ. 5.6 for a time-dependent frequency, we first re-write it:

$$\frac{d}{dt}\mu_{01}(t) = -i\omega\mu_{01}(t) \tag{5.8}$$

and replace it by:

$$\frac{d}{dt}\mu_{01}(t) = -i\omega(t)\mu_{01}(t) \tag{5.9}$$

which yields:

$$\mu_{01}(t) = e^{-i\int_0^t d\tau\omega(\tau)}\mu_{01}(0) \tag{5.10}$$

We separate the frequency into its time average and a fluctuating part:

$$\omega(t) = \omega + \delta\omega(t) \tag{5.11}$$

with $\omega \equiv \langle\omega(t)\rangle$ and $\langle\delta\omega(t)\rangle \equiv 0$ where, $\langle\ldots\rangle$ denotes time and/or ensemble averaging (which both are the same). An example of a fluctuating transition frequency is depicted in the following picture:

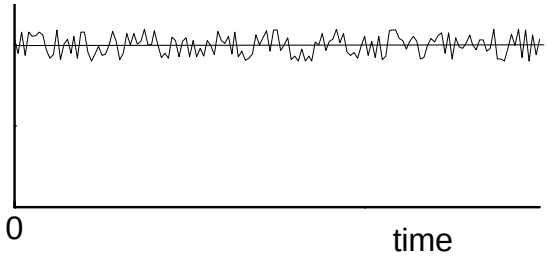

The linear response function is give by:

$$\langle \mu_{01}(t)\,\mu_{10}(0)\,\rho_{00}\rangle = \mu_{01}^2 e^{-i\omega t}\left\langle \exp\left(-i\int_0^t d\tau\delta\omega(\tau)\right)\right\rangle \tag{5.12}$$

This expression is commonly calculated using the cummulant expansion. To this end, we expand the exponential function in powers of $\delta\omega$ (which is assumed to be small).

$$\begin{aligned}\left\langle \exp\left(-i\int_0^t d\tau\delta\omega(\tau)\right)\right\rangle &= 1 - i\int_0^t d\tau\,\langle\delta\omega(\tau)\rangle \\ &\quad -\frac{1}{2}\int_0^t\int_0^t d\tau' d\tau''\,\langle\delta\omega(\tau')\,\delta\omega(\tau'')\rangle + \ldots\end{aligned} \tag{5.13}$$

The linear term vanishes by definition

$$\left\langle \exp\left(-i\int_0^t d\tau\delta\omega(\tau)\right)\right\rangle = 1 - \frac{1}{2}\int_0^t\int_0^t d\tau' d\tau''\,\langle\delta\omega(\tau')\,\delta\omega(\tau'')\rangle + \ldots \tag{5.14}$$

We postulate that we can write this expression in the following form:

$$\left\langle \exp\left(-i\int_0^t d\tau\delta\omega(\tau)\right)\right\rangle \equiv e^{-g(t)} = 1 - g(t) + \frac{1}{2}g^2(t) + \ldots \tag{5.15}$$

and expand $g(t)$ in powers of $\delta\omega$:

$$g(t) = g_1(t) + g_2(t) + \ldots \tag{5.16}$$

where $g_1(t)$ is of the order $O(\delta\omega)$, g_2 of the order $O(\delta\omega^2)$ and so on. Inserting Equ. 5.15 into Equ. 5.16 and ordering the terms in powers of $\delta\omega$ yields:

$$e^{-g(t)} = 1 - (g_1(t) + g_2(t) + \ldots) + \frac{1}{2}(g_1(t) + g_2(t) + \ldots)^2 \tag{5.17}$$

The linear term vanishes by construct, so that we find $g_1(t) = 0$ and the leading term is quadratic in $\delta\omega$. Hence, we obtain for the so-called *lineshape function* $g(t)$:

$$g\left(t\right) \equiv g_2(t) = \frac{1}{2}\int_0^t\int_0^t d\tau' d\tau'' \left\langle \delta\omega\left(\tau'\right)\delta\omega\left(\tau''\right)\right\rangle + O(\delta\omega^3) \tag{5.18}$$

Since the correlation function $\left\langle \delta\omega\left(\tau'\right)\delta\omega\left(\tau''\right)\right\rangle$ in equilibrium depends only on the time interval τ'-τ", the correlation function can be replaced by $\left\langle \delta\omega\left(\tau'-\tau''\right)\delta\omega\left(0\right)\right\rangle$.

Remarks:

- The cummulant expansion is just an intelligent way of reordering terms of different powers of $\delta\omega$, which is of course in general not exact in all orders of $\delta\omega$. However, one can show that the second order cummulant is exact when the distribution of $\delta\omega$ is Gaussian. According to the central limit theorem this is often the case to a very good approximation, namely when the random property $\delta\omega$ is a sum of many different random influences (like a molecule in a bath, which is affected by many bath molecules surrounding it)
- The cummulant expansion effectively shift the averaging from $\left\langle e^{-i\int\cdots}\right\rangle \approx e^{-\int\langle\cdots\rangle}$, which is much simpler to calculate in practice.

To summarize (see also Equ. 4.10):

$$A(\omega) = 2\Re\int_0^\infty dt e^{i\omega t}\left\langle\mu_{01}(t)\mu_{10}(0)\right\rangle = 2\mu_{01}^2\Re\int_0^\infty dt e^{i\omega t}e^{-g(t)} \tag{5.19}$$

with

$$\begin{aligned} g\left(t\right) &= \frac{1}{2}\int_0^t\int_0^t d\tau' d\tau'' \left\langle \delta\omega\left(\tau'-\tau''\right)\delta\omega\left(0\right)\right\rangle \\ &= \int_0^t\int_0^{\tau'} d\tau' d\tau'' \left\langle \delta\omega\left(\tau''\right)\delta\omega\left(0\right)\right\rangle \end{aligned} \tag{5.20}$$

For the last step we have used that $\langle\delta\omega(\tau)\delta\omega(0)\rangle = \langle\delta\omega(-\tau)\delta\omega(0)\rangle$ is symmetric in time. The two-point correlation function $\left\langle \delta\omega\left(t\right)\delta\omega\left(0\right)\right\rangle$ describes all linear spectroscopy (in the limits of the cummulant expansion).

When the transition frequency fluctuations are very fast, the frequency shift at time 0, $\delta\omega(0)$, is uncorrelated with that a short time later. In that case, the correlation function $\langle \delta\omega(t)\,\delta\omega(0)\rangle$ will decay very quickly and can be approximated by a δ-function: $\langle \delta\omega(t)\,\delta\omega(0)\rangle \rightarrow \delta(t)$. However, we often find the following situation: When the frequency is at some value at time 0, it will stay in the neighborhood of this frequency for quite some time and loose the memory about this frequency only after some time. The following picture shows an example:

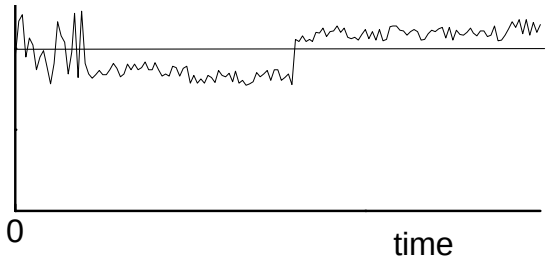

In that case, the correlation function $\langle \delta\omega(t)\,\delta\omega(0)\rangle$ will decay slowly in time. It is often modelled by an exponential function,:

$$\langle \delta\omega(t)\,\delta\omega(0)\rangle = \Delta^2 e^{-\frac{|t|}{\tau_c}} \tag{5.21}$$

which depends on two parameters, the fluctuation amplitude Δ and the correlation time τ_c. Integrating the correlation function twice reveals for the *Kubo-lineshape* function:

$$g(t) = \Delta^2\tau_c^2\left[e^{-\frac{t}{\tau_c}} + \frac{t}{\tau_c} - 1\right] \tag{5.22}$$

This model is well suited to discuss different limits:

$\Delta\tau_c << 1$, the *fast modulation, motional narrowing* or *homogeneous* limit:

In this limit, we obtain for the line shape function:

$$g(t) = t/T_2 \tag{5.23}$$

with $T_2 = (\Delta^2\tau_c)^{-1}$

This is since we have $e^{-\frac{t}{\tau_c}} \rightarrow 0$ and $\frac{t}{\tau_c} >> 1$

The absorption spectrum:

$$A(\omega) = \Re\int_0^\infty e^{i\omega t}e^{-g(t)}dt = \Re\int_0^\infty e^{i\omega t}e^{-t/T_2}dt \tag{5.24}$$

yields a Lorentzian line with homogeneous width T_2^{-1}. This limit applies for $\Delta\tau_c << 1$ or $\tau_c << T_2$

$\Delta\tau_c >> 1$, the *slow modulation* or *inhomogeneous* limit:

In that case we get for the line shape function

$$g(t) = \frac{\Delta^2}{2}t^2 \tag{5.25}$$

which can be seen when expanding the exponential function in Equ. 5.21. The line shape function is independent on the correlation time τ_c. The absorption spectrum

$$A(\omega) = \Re \int_0^\infty e^{i\omega t} e^{-g(t)} dt = \Re \int_0^\infty e^{i\omega t} e^{-\frac{\Delta^2}{2}t^2} dt \tag{5.26}$$

yields a Gaussian line with width Δ. This limit applies for $\Delta\tau_c >> 1$

Hence, we see that the width of an absorption line is given by the width of the distribution of $\delta\omega$ whenever the fluctuations are slow enough. However, when increasing the rate of the fluctuations, we reach the fast modulation limit and obtain a Lorentzian line. The line width then is getting narrower (since $T_2^{-1} = \Delta^2\tau_c << \Delta$) and decreases linearly with the correlation time τ_c. This phenomenon is called motional narrowing. The following picture shows this effect for a constant fluctuation amplitude Δ and different values for the parameter $\Delta \cdot \tau_c$.

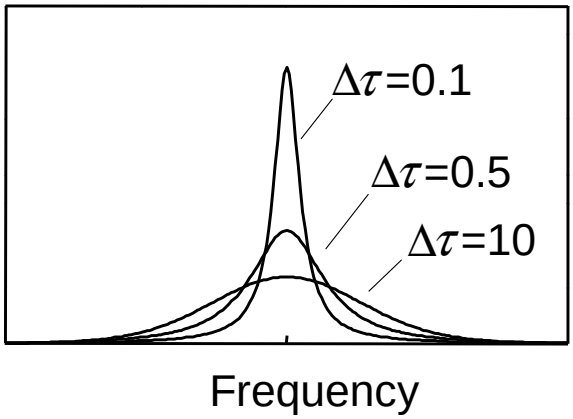

5.2 Nonlinear Response

We can develop the nonlinear response functions along the same lines. For a 2-level system, the following 4 Feynman diagrams are possible within the rotating wave ap-

proximation:

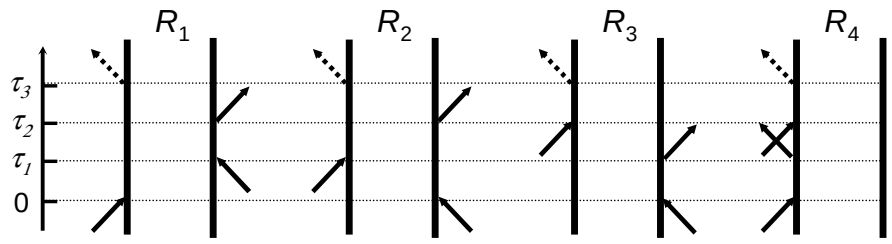

Let's develop the response function R_1 with the same rules as in the previous paragraph:

$$R_1(\tau_3, \tau_2, \tau_1) = -\left(\frac{i}{\hbar}\right)^3 \langle \mu_{01}(\tau_3)\mu_{10}(0)\rho_{00}\mu_{01}(\tau_1)\mu_{10}(\tau_2)\rangle \tag{5.27}$$

where we switched back to absolute time points, rather than time intervals:

$$\begin{aligned} \tau_1 &= t_1 \\ \tau_2 &= t_2 + t_1 \\ \tau_3 &= t_3 + t_2 + t_1 \end{aligned} \tag{5.28}$$

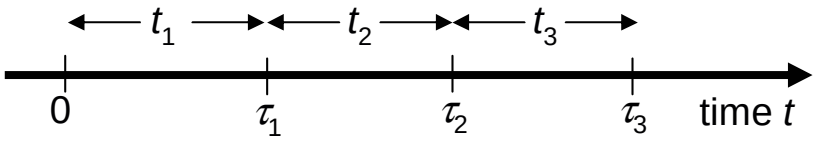

Using the sign-rules developed in the last paragraph (i.e. $\mu_{01}(t) = e^{-i\omega t}\mu_{01}$ and $\mu_{10}(t) = e^{+i\omega t}\mu_{10}$), we obtain

$$\begin{aligned} R_1(\tau_3, \tau_2, \tau_1) \;=\; & -\left(\frac{i}{\hbar}\right)^3 \mu^4 e^{-i\omega(\tau_3 - \tau_2 + \tau_1)} \\ & \left\langle \exp\left[-i\int_0^{\tau_3}\delta\omega(\tau)d\tau + i\int_0^{\tau_2}\delta\omega(\tau)d\tau - i\int_0^{\tau_1}\delta\omega(\tau)d\tau\right]\right\rangle \end{aligned} \tag{5.29}$$

We again calculate this expression using the cummulant expansion. To this end, we

expand the exponential function up to second powers of $\delta\omega$

$$\begin{aligned}\langle\cdots\rangle &= 1-\frac{1}{2}\int_0^{\tau_3}\int_0^{\tau_3}\langle\delta\omega(\tau'')\delta\omega(\tau')\rangle\,d\tau''d\tau' - \frac{1}{2}\int_0^{\tau_2}\int_0^{\tau_2}\langle\delta\omega(\tau'')\delta\omega(\tau')\rangle\,d\tau''d\tau' \\ &-\frac{1}{2}\int_0^{\tau_1}\int_0^{\tau_1}\langle\delta\omega(\tau'')\delta\omega(\tau')\rangle\,d\tau''d\tau' - \int_0^{\tau_3}\int_0^{\tau_1}\langle\delta\omega(\tau'')\delta\omega(\tau')\rangle\,d\tau''d\tau' \\ &+\int_0^{\tau_3}\int_0^{\tau_2}\langle\delta\omega(\tau'')\delta\omega(\tau')\rangle\,d\tau''d\tau' + \int_0^{\tau_2}\int_0^{\tau_1}\langle\delta\omega(\tau'')\delta\omega(\tau')\rangle\,d\tau''d\tau' + O(\delta\omega^3)\end{aligned} \tag{5.30}$$

The terms linear in $\delta\omega$ vanish by construct. The first three terms are the line shape functions $g(\tau)$ at times τ_3, τ_2, and τ_1. We write Equ. 5.30 in the form:

$$\langle\cdots\rangle = 1 - g(\tau_3) - g(\tau_2) - g(\tau_1) - h(\tau_3,\tau_1) + h(\tau_3,\tau_2) + h(\tau_2,\tau_1) + O(\delta\omega^3) \tag{5.31}$$

Realizing that the functions $h(\tau',\tau)$ contain the same integrand as $g(\tau)$, and are different only by the integration limits, we find, for example:

$$h(\tau_2,\tau_1) = g(\tau_2) + g(\tau_1) - g(\tau_2-\tau_1) \tag{5.32}$$

We see that from the following figure, which shows the integration areas:

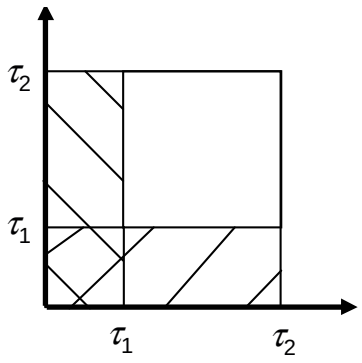

where both shaded rectangulars corresponds to $2h(\tau_2,\tau_1)$, the lower left square to $2g(\tau_1)$, the total square to $2g(\tau_2)$ and the upper right square to $2g(\tau_2-\tau_1)$. Hence, we obtain:

$$\begin{aligned}\langle\cdots\rangle = 1 - g(\tau_3) + g(\tau_2) - g(\tau_1) + g(\tau_3-\tau_1) - g(\tau_3-\tau_2) - g(\tau_2-\tau_1) \\ +O(\delta\omega^3)\end{aligned} \tag{5.33}$$

or, when switching back to the time intervals t_1, t_2 and t_3 (see Equ. 5.28)

$$\langle \cdots \rangle = 1 - g(t_1) - g(t_2) - g(t_3) + g(t_1 + t_2) + g(t_2 + t_3) - g(t_1 + t_2 + t_3) + O(\delta\omega^3) \quad (5.34)$$

We postulate

$$\langle \cdots \rangle = e^{-f} \quad (5.35)$$

Expanding f in powers of $\delta\omega$ and collecting the terms of different powers of $\delta\omega$ yields for the nonlinear response function:

$$R_1(t_3, t_2, t_1) = -\left(\frac{i}{\hbar}\right)^3 \mu^4 e^{-i\omega(t_1+t_3)} e^{-g(t_1)-g(t_2)-g(t_3)+g(t_1+t_2)+g(t_2+t_3)-g(t_1+t_2+t_3)} \quad (5.36)$$

Likewise, we obtain for R_2:

$$R_2(\tau_3, \tau_2, \tau_1) = -\left(\frac{i}{\hbar}\right)^3 \langle \mu_{01}(\tau_3)\mu_{10}(\tau_1)\rho_{00}\mu_{01}(0)\mu_{10}(\tau_2)\rangle \quad (5.37)$$

$$= -\left(\frac{i}{\hbar}\right)^3 \mu^4 e^{-i\omega(\tau_3-\tau_2-\tau_1)} \left\langle \exp\left[-i\int_0^{\tau_3}\delta\omega(\tau)d\tau + i\int_0^{\tau_2}\delta\omega(\tau)d\tau + i\int_0^{\tau_1}\delta\omega(\tau)d\tau\right]\right\rangle$$

This expression has the same structure as R_1, except for the signs of the oscillatory part. We calculate it along the same lines as R_1 and obtain:

$$R_2(t_3, t_2, t_1) = -\left(\frac{i}{\hbar}\right)^3 \mu^4 e^{-i\omega(t_3-t_1)} e^{-g(t_1)+g(t_2)-g(t_3)-g(t_1+t_2)-g(t_2+t_3)+g(t_1+t_2+t_3)} \quad (5.38)$$

The diagram R_3:

$$R_3(\tau_3, \tau_2, \tau_1) = -\left(\frac{i}{\hbar}\right)^3 \langle \mu_{01}(\tau_3)\mu_{10}(\tau_2)\rho_{00}\mu_{01}(0)\mu_{10}(\tau_1)\rangle \quad (5.39)$$

$$= -\left(\frac{i}{\hbar}\right)^3 \mu^4 e^{-i\omega(\tau_3-\tau_2-\tau_1)} \left\langle \exp\left[-i\int_0^{\tau_3}\delta\omega(\tau)d\tau + i\int_0^{\tau_2}\delta\omega(\tau)d\tau + i\int_0^{\tau_1}\delta\omega(\tau)d\tau\right]\right\rangle$$

$$= R_2(\tau_3, \tau_2, \tau_1)$$

yields the same response as R_2. R_4 is:

$$\begin{aligned} R_4(\tau_3,\tau_2,\tau_1) &= -\left(\frac{i}{\hbar}\right)^3 \langle \mu_{01}(\tau_3)\mu_{10}(\tau_2)\mu_{01}(\tau_1)\mu_{10}(0)\rho_{00}\rangle \\ &= \left(\frac{i}{\hbar}\right)^3 \mu^4 e^{-i\omega(\tau_3-\tau_2+\tau_1)} \left\langle \exp\left[-i\int_0^{\tau_3}\delta\omega(\tau)d\tau + i\int_0^{\tau_2}\delta\omega(\tau)d\tau - i\int_0^{\tau_1}\delta\omega(\tau)d\tau\right]\right\rangle \\ &= R_1(\tau_3,\tau_2,\tau_1) \end{aligned} \tag{5.40}$$

which is the same as R_1.

We summarize the final result:

$$\begin{aligned} R_1(t_3,t_2,t_1) &= -\left(\frac{i}{\hbar}\right)^3 \mu^4 e^{-i\omega(t_1+t_3)} e^{-g(t_1)-g(t_2)-g(t_3)+g(t_1+t_2)+g(t_2+t_3)-g(t_1+t_2+t_3)} \\ R_2(t_3,t_2,t_1) &= -\left(\frac{i}{\hbar}\right)^3 \mu^4 e^{-i\omega(t_3-t_1)} e^{-g(t_1)+g(t_2)-g(t_3)-g(t_1+t_2)-g(t_2+t_3)+g(t_1+t_2+t_3)} \\ R_3(t_3,t_2,t_1) &= -\left(\frac{i}{\hbar}\right)^3 \mu^4 e^{-i\omega(t_3-t_1)} e^{-g(t_1)+g(t_2)-g(t_3)-g(t_1+t_2)-g(t_2+t_3)+g(t_1+t_2+t_3)} \\ R_4(t_3,t_2,t_1) &= -\left(\frac{i}{\hbar}\right)^3 \mu^4 e^{-i\omega(t_1+t_3)} e^{-g(t_1)-g(t_2)-g(t_3)+g(t_1+t_2)+g(t_2+t_3)-g(t_1+t_2+t_3)} \end{aligned} \tag{5.41}$$

Note that the equalities $R_1 = R_4$ and $R_2 = R_3$ hold only within the framework of the stochastic ansatz of Kubo's line shape theory and will no longer be true in the Brownian oscillator model (see Sec. 6). The response functions R_1 to R_4 describe all nonlinear spectroscopy of a 2-level system in terms of the two-point frequency fluctuation correlation function $\langle \delta\omega(\tau)\,\delta\omega(0)\rangle$. This frequency fluctuation correlation function describes the influence of the bath on the system.

5.3 Three-Pulse Photon Echo Spectroscopy

Homogeneous and inhomogeneous broadening can be obtained from the frequency fluctuation correlation function $\langle \delta\omega(\tau)\,\delta\omega(0)\rangle$ as limiting cases. Homogeneous and inhomogeneous broadening imply a strict separation of timescales, the first being infinitely fast and the second being infinitely slow. Hence the frequency fluctuation correlation function corresponding to a inhomogeneous distribution of homogeneous lines is:

$$\langle \delta\omega(t)\,\delta\omega(0)\rangle = \Gamma\delta(t) + \Delta_0^2/2 \tag{5.42}$$

and for the line shape function:

$$g(t) = \Gamma t + \Delta_0^2 t^2 \tag{5.43}$$

This is the so-called *Voigt profile*, i.e. a Lorentzian line shape convoluted with a Gaussian distribution. When inserting this line shape function for example into R_2, we obtain:

$$R_2(t_3, t_2, t_1) = -\left(\frac{i}{\hbar}\right)^3 \mu^4 e^{-i\omega(t_3-t_1)} e^{-\Gamma(t_3+t_1)} e^{-\Delta_0^2(t_3-t_1)^2} \tag{5.44}$$

This is the same expression as Equ. 4.31, where we have described dephasing phenomenologically. Note that the response function is independent on t_2. In other words, as long as there is a strict separation of timescales of homogeneous and inhomogeneous broadening, there is no need to experimentally control the delay time t_2. In a two-pulse photon echo experiment, the time $t_2$is implicitly set to zero, since the second and third interaction come from one, short pulse.

In general there will be no strict separation of timescales of homogeneous and inhomogeneous broadening. This is in particular true in solution phase systems, which fluctuate on a wide range of time scales, and a *Kubo line shape* is a much more realistic model for the frequency fluctuation correlation function:

$$\langle \delta\omega\,(t)\,\delta\omega\,(0)\rangle = \Delta^2 e^{-\frac{|t|}{\tau_C}} \tag{5.45}$$

In that case, the response functions $R_1 - R_4$ do in fact depend on t_2. If we want to measure these phenomena, one needs an experimental technique to control that delay time. The technique of choice to control all time delays is the three-pulse photon echo experiment with the geometry:

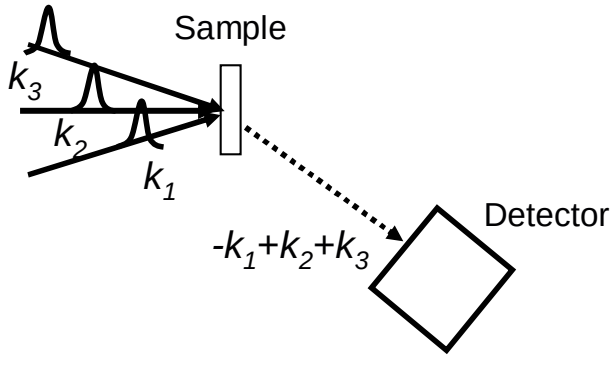

The detector is put in the direction $-k_1 + k_2 + k_3$, which implies that we select only diagram R_2 and R_3 (which both yield the same response). An example of such a measurement is shown in the following picture:

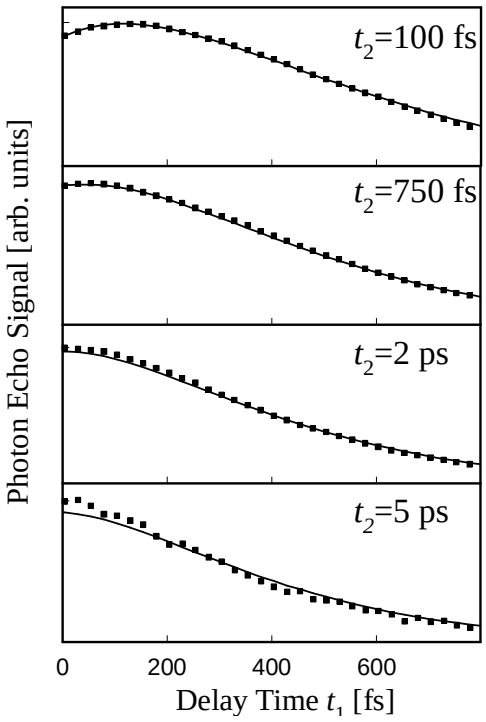

The figure shows the photon echo response of the asymmetric stretching frequency of N_3^- in H_20 as a function of t_1 and t_2. For early times t_2, we observe a peak shift as a function of t_1, which we have already discussed in Sec. 4.4. The peak shift is a measure of the inhomogeneity. However, since the inhomogeneity is not static (the solvent is constantly rearranging), the peak shift resembles inhomogeneity still present at time t_2. The inhomogeneity decays as function of time, observed as a decay of the peak shift. When plotting the peak shift as a function of time t_2:

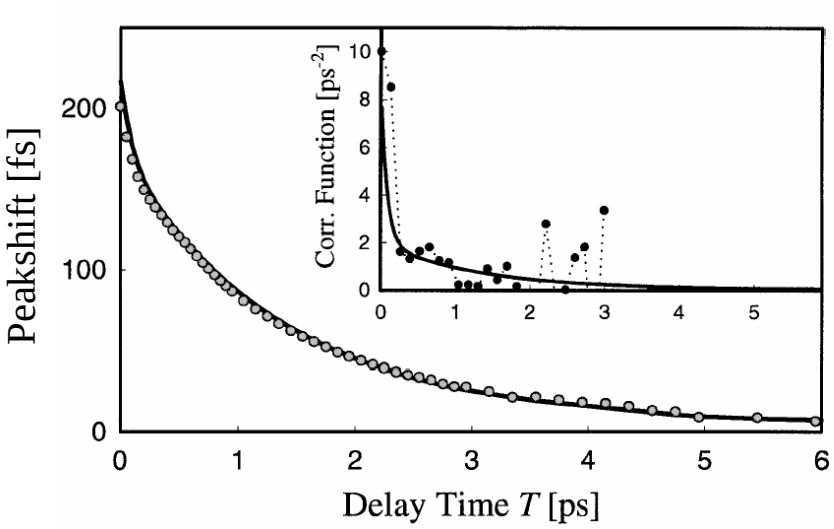

one obtains a quantity which resemble the frequency fluctuation correlation function

$\langle \delta\omega(\tau)\,\delta\omega(0)\rangle$ (see insert, solid line). This is the essential property deduced from a *photon echo peak shift* experiment.

As a result of truncating the cummulant expansion after second order, the nonlinear response function $R_1 - R_4$ are completely desctribed by the line shape function $g(t)$, i.e. by the two-point frequency fluctuation correlation function $\langle \delta\omega(\tau)\,\delta\omega(0)\rangle$. In other words, the information contents of a linear experiment and any 3^{rd} order experiment seem to be the same. One could in principle measure the frequency fluctuation correlation function $\langle \delta\omega(\tau)\,\delta\omega(0)\rangle$ by measuring just the linear absorption spectrum and inverting Equ. 5.19, and it seems there is no need to apply nonlinear spectroscopy. In practice, however, this is very difficult and yields poor results. The dotted line in the insert of the above picture is the frequency fluctuation correlation function $\langle \delta\omega(\tau)\,\delta\omega(0)\rangle$ determined in that way. It does in fact resemble that determined from the photon echo experiment but is by far noisier.

6 Microscopic Theory of Dephasing: Brownian Oscillator Model

6.1 Time Evolution Operator of a Time Dependent Hamiltonian

In contrast to Kubo's lineshape theory, which is a classical theory, the Brownian Oscillator Model is fully quantum mechanical. In order to introduce the Brownian Oscillator Model, we have to revisit the concept of the time evolution operator, now for a time dependent Hamiltonian. The time evolution operator was defined in Sec. 2.2 as:

$$|\psi(t)\rangle \equiv U(t,t_0)\,|\psi(t_0)\rangle \tag{6.1}$$

and we have seen that it is:

$$U_0(t,t_0) = e^{-\frac{i}{\hbar}H\cdot(t-t_0)} \tag{6.2}$$

This is true only when H is time-independent! For a time-dependent Hamiltonian, we insert Equ. 6.1. into the Schrödinger equation:

$$\frac{d}{dt}\left(U(t,t_0)\,|\psi(t_0)\rangle\right) = -\frac{i}{\hbar}H(t)\cdot U(t,t_0)\,|\psi(t_0)\rangle \tag{6.3}$$

with a time-dependent Hamiltonian. Since this equation must hold for any starting wave function $|\psi(t_0)\rangle$, we get:

$$\frac{d}{dt}U(t,t_0) = -\frac{i}{\hbar}H(t)\cdot U(t,t_0) \tag{6.4}$$

Integrating this equation yields:

$$U(t,t_0) = 1 - \frac{i}{\hbar}\int_{t_0}^{t} d\tau H(\tau)\cdot U(\tau,t_0) \tag{6.5}$$

which can be solved by plugging it into itself iteratively:

$$U(t,t_0) = 1 + \sum_{n=1}^{\infty}\left(-\frac{i}{\hbar}\right)^n \int_{t_0}^{t} d\tau_n \int_{t_0}^{\tau_n} d\tau_{n-1}\ldots\int_{t_0}^{\tau_2} d\tau_1 H(\tau_n)H(\tau_{n-1})\ldots H(\tau_1) \tag{6.6}$$

Note that this is a time-ordered integral with

$$\tau_1 \leq \tau_2 \leq \ldots \leq \tau_n \tag{6.7}$$

If we had ignored that $H(t)$ is an operator and treated it as a function, we could have solved Equ. 6.4 by:

$$U(t,t_0) \stackrel{?}{=} \exp\left[-\frac{i}{\hbar}\int_{t_0}^{t} d\tau H(\tau)\right] \tag{6.8}$$

Expanding the exponential function would yield:

$$U(t,t_0) \stackrel{?}{=} 1 + \sum_{n=1}^{\infty} \frac{1}{n!}\left(-\frac{i}{\hbar}\right)^n \int_{t_0}^{t} d\tau_n \int_{t_0}^{t} d\tau_{n-1} \ldots \int_{t_0}^{t} d\tau_1 H(\tau_n)H(\tau_{n-1})\ldots H(\tau_1) \tag{6.9}$$

which is very similar as Equ. 6.6, but is wrong. The essential difference is the fact that the time variables are not ordered in Equ. 6.9. The difference is illustrated in the following representation of the integration area (i.e. the shaded areas):

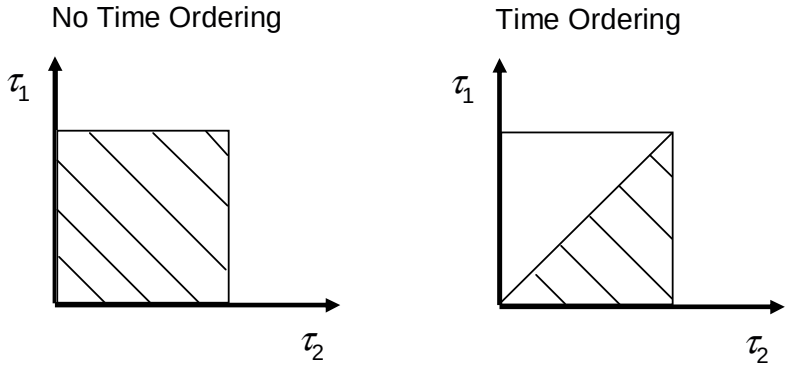

If we had:

$$H(\tau_1)H(\tau_2) \stackrel{?}{=} H(\tau_2)H(\tau_1) \tag{6.10}$$

which of course would be true if $H(t)$ would be an ordinary function, then the non-time-ordered integration would yield the same result for the upper-left triangle and the lower-right triangle. In that case, Equ. 6.6 and Equ. 6.9 would in fact be equivalent (the factor $1/n!$ in Equ. 6.9 takes care of the multiple treatment of identical terms).

However, $H(t)$ is an operator, and $H(\tau_1)$ and $H(\tau_2)$ do in general not commute (except when H is not time dependent):

$$[H(\tau_1)H(\tau_2)] \neq 0 \tag{6.11}$$

This is why both expression Equ. 6.6 and 6.9 are different. Nevertheless, in order to emphasize the similarity of Equ. 6.6 and an exponential function, we define a positive time ordered exponential:

$$\exp_+\left[-\frac{i}{\hbar}\int_{t_0}^{t} d\tau H(\tau)\right] \equiv 1 \quad + \quad \sum_{n=1}^{\infty}\left(-\frac{i}{\hbar}\right)^n \int_{t_0}^{t} d\tau_n \ldots \int_{t_0}^{\tau_2} d\tau_1 H(\tau_n)\ldots H(\tau_1) \tag{6.12}$$

and obtain for the time evolution operator of a time dependent Hamiltonian:

$$U(t,t_0) = \exp_+\left[-\frac{i}{\hbar}\int_{t_0}^{t} d\tau H(\tau)\right] \tag{6.13}$$

Likewise, the negative time ordered exponential is defined as:

$$\exp_-\left[+\frac{i}{\hbar}\int_{t_0}^{t} d\tau H(\tau)\right] \equiv 1 \quad + \quad \sum_{n=1}^{\infty}\left(+\frac{i}{\hbar}\right)^n \int_{t_0}^{t} d\tau_n \ldots \int_{t_0}^{\tau_2} d\tau_1 H(\tau_1)\ldots H(\tau_n) \tag{6.14}$$

which is the adjunct of the time evolution operator:

$$U^\dagger(t,t_0) = \exp_-\left[+\frac{i}{\hbar}\int_{t_0}^{t} d\tau H(\tau)\right] \tag{6.15}$$

We often will have

$$H = H^{(0)} + H' \tag{6.16}$$

where $H^{(0)}$ is a system operator and H' a (hopefully small) perturbation. Applying the definition of the time ordered exponentials, we obtain the following rule:

$$e^{-\frac{i}{\hbar}\left(H^{(0)}+H'\right)t} = e^{-\frac{i}{\hbar}H^{(0)}t}\exp_+\left[-\frac{i}{\hbar}\int_{t_0}^{t} d\tau H'(\tau)\right] \tag{6.17}$$

with $H'(\tau)$ being the Hamiltonian H' in the interaction picture with respect to $H^{(0)}$:

$$H'(\tau) = e^{\frac{i}{\hbar}H^{(0)}t} H' e^{-\frac{i}{\hbar}H^{(0)}t} \tag{6.18}$$

6.2 Brownian Oscillator Model

The Kubo Model assumed a fluctuating transition frequency, caused by the solvent, but did not specify how the solvent couples to the transition. The Brownian Oscillator model does exactly specify the coupling. It assumes a set of electronic states, whose energies depend on a set of nuclear coordinates q as parameters (this is the Born Oppenheimer approximation). Typically, one assumes that the potential surfaces are harmonic:

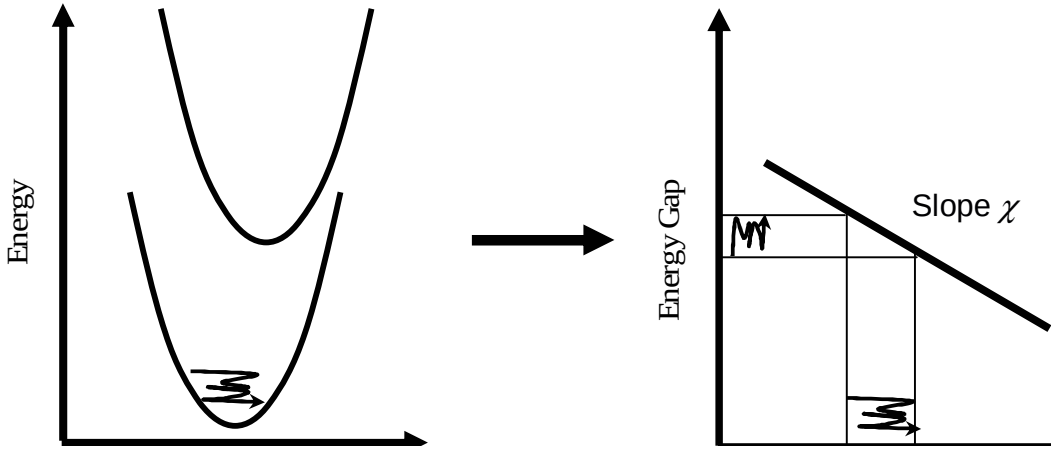

When the harmonic potential surfaces of the ground and the excited states are displaced, the energy gap between the ground and the excited state will vary linearly with the nuclear coordinate q. A fluctuating coordinate due to thermal excitation of the nuclear coordinates hence will give rise to a fluctuating transition frequency. In that sense the Brownian oscillator model is a more microscopic model, which specifies the reason for a fluctuating transition frequency.

Within the Born Oppenheimer approximation, one can write the total wave function as a product of an electronic and a nuclear wave function (i.e. one can separate the electronic from the nuclear problem):

$$\Psi = \Psi_{el}\Psi_{nuc} \tag{6.19}$$

The Hamiltonian again is:

$$H = H_s + E(t)\mu \tag{6.20}$$

where the system Hamiltonian is now the electronic plus the nuclear problem. We expand the Hamiltonian with respect to the electronic eigenstates (assuming it is an electronic two-level system):

$$H_s = |0\rangle H_0 \langle 0| + |1\rangle H_1 \langle 1| \tag{6.21}$$

One remark on the notation: H_0 and H_1 are now eigenvalues (numbers) with respect to the electronic problem, but they are still operators with respect to the nuclear problem. For linear response, we have to calculate the dipole-dipole correlation function:

$$\langle \mu(t)\mu(0)\rho(-\infty)\rangle \tag{6.22}$$

which, when we expand it with respect to the electronic system is (see Equ. 5.5):

$$\langle \mu_{01}(t)\mu_{10}(0)\rho(-\infty)\rangle \tag{6.23}$$

Note that $\mu_{01}(t)$ is still an operator with respect to the nuclear problem. The notation $\mu_{01}(t)$

$$\mu_{01}(t) = e^{\frac{i}{\hbar}H_0 t}\mu_{01}e^{-\frac{i}{\hbar}H_1 t} \tag{6.24}$$

denotes the dipole operator μ time-propagated with respect to H_0 on the left side and with respect to H_1 on the right side. For convenience, we want to express Equ. 6.24 with respect to one Hamiltonian, a reference Hamiltonian, for which we choose H_0. To this end, we introduce the energy gap operator $\Omega \equiv H_1 - H_0 - (\varepsilon_1 - \varepsilon_0)$:

$$H_1 \equiv H_0 + \Omega + (\varepsilon_1 - \varepsilon_0) \tag{6.25}$$

We included the average energy gap $(\varepsilon_1 - \varepsilon_0)$ (which is just numbers, not operators), to separate off the quickly oscillating part from the energy gap operator Ω. Then, we get for

$$\begin{aligned} \mu_{01}(t) &= e^{\frac{i}{\hbar}H_0 t}\mu e^{-\frac{i}{\hbar}H_1 t} \\ &= e^{-\frac{i}{\hbar}(\varepsilon_1-\varepsilon_0)t}e^{\frac{i}{\hbar}H_0 t}\mu e^{-\frac{i}{\hbar}(H_0+\Omega)t} \\ &= e^{-\frac{i}{\hbar}(\varepsilon_1-\varepsilon_0)t}e^{\frac{i}{\hbar}H_0 t}\mu e^{-\frac{i}{\hbar}H_0 t}\exp_+\left(-\frac{i}{\hbar}\int_0^t \Omega(\tau)d\tau\right) \end{aligned} \tag{6.26}$$

with

$$\Omega(\tau) = e^{\frac{i}{\hbar}H_0\tau}\Omega e^{-\frac{i}{\hbar}H_0\tau} \tag{6.27}$$

the energy gap operator in the interaction picture with respect to the ground state Hamiltonian H_0. We have used Equ. 6.17 in the last step. Equ. 6.26 contains the dipole operator in the interaction picture with respect to ground state Hamiltonian H_0:

$$\mu(t) = e^{\frac{i}{\hbar}H_0 t}\mu e^{-\frac{i}{\hbar}H_0 t} \tag{6.28}$$

At this point, we adopt the Franck-Condon approximation which assumes that the dipole moment $\mu(t)$ of the molecule does not depend on nuclear coordinate q and is a constant μ. In other words, even though q is a fluctuation property, the dipole operator $\mu(t)$ will be constant in time and can be replaced by a number. Hence, we get:

$$\mu_{01}(t) = \mu e^{-\frac{i}{\hbar}(\varepsilon_1-\varepsilon_0)t}\exp_+\left(-\frac{i}{\hbar}\int_0^t \Omega(\tau)d\tau\right) \tag{6.29}$$

We get along the same lines:

$$\mu_{10}(t) = \mu e^{+\frac{i}{\hbar}(\varepsilon_1-\varepsilon_0)t}\exp_-\left(+\frac{i}{\hbar}\int_0^t \Omega(\tau)d\tau\right) \tag{6.30}$$

The linear response function is:

$$\langle\mu_{01}(t)\mu_{10}(0)\rho(-\infty)\rangle = \mu^2 e^{-\frac{i}{\hbar}(\varepsilon_1-\varepsilon_0)t}\left\langle\exp_+\left(-\frac{i}{\hbar}\int_0^t \Omega(\tau)d\tau\right)\right\rangle \tag{6.31}$$

which is the equivalent of Equ. 5.12 in Kubo's line shape theory:

$$\langle\mu_{01}(t)\,\mu_{10}(0)\rangle = \mu^2 e^{-i\omega t}\left\langle\exp\left(-i\int_0^t d\tau\delta\omega(\tau)\right)\right\rangle \tag{6.32}$$

The essential difference is that the integrand in Equ. 6.31 is a quantum mechanical operator in the Brownian oscillator model, rather than an ordinary function in Kubo's line shape theory. As a result, the exponential function is a time-ordered exponential. We nevertheless can perform the cummulant expansion in exactly the same way as in Sec. 5, keeping in mind that the operators do not commute and that the exponential functions are time-ordered exponentials. We then get for the linear absorption spectrum:

$$A(\omega) = 2Re\int_0^\infty dt e^{i\omega t}\langle\mu_{01}(t)\mu_{10}(0)\rho(-\infty)\rangle = 2\mu^2 Re\int_0^\infty dt e^{i\omega t}e^{-g(t)} \tag{6.33}$$

with

$$g\left(t\right)=\frac{1}{\hbar^{2}}\int\limits_{0}^{t}d\tau''\int\limits_{0}^{\tau''}d\tau'\left\langle \Omega\left(\tau'\right)\Omega\left(0\right)\rho\left(-\infty\right)\right\rangle \tag{6.34}$$

Note that the line shape function $g(t)$ now is a time-ordered integral τ'$\leq\tau$"$\leq$t, in contrast to Equ. 5.20. We obtain for the nonlinear response functions:

$$\begin{aligned}
R_{1}(t_{3},t_{2},t_{1}) &= -\left(\frac{i}{\hbar}\right)^{3}\mu^{4}e^{-i\omega(t_{1}+t_{3})}e^{-g(t_{1})-g^{*}(t_{2})-g^{*}(t_{3})+g(t_{1}+t_{2})+g^{*}(t_{2}+t_{3})-g(t_{1}+t_{2}+t_{3})}\\
R_{2}(t_{3},t_{2},t_{1}) &= -\left(\frac{i}{\hbar}\right)^{3}\mu^{4}e^{-i\omega(t_{3}-t_{1})}e^{-g^{*}(t_{1})+g(t_{2})-g^{*}(t_{3})-g^{*}(t_{1}+t_{2})-g(t_{2}+t_{3})+g^{*}(t_{1}+t_{2}+t_{3})}\\
R_{3}(t_{3},t_{2},t_{1}) &= -\left(\frac{i}{\hbar}\right)^{3}\mu^{4}e^{-i\omega(t_{3}-t_{1})}e^{-g^{*}(t_{1})+g^{*}(t_{2})-g(t_{3})-g^{*}(t_{1}+t_{2})-g^{*}(t_{2}+t_{3})+g^{*}(t_{1}+t_{2}+t_{3})}\\
R_{4}(t_{3},t_{2},t_{1}) &= -\left(\frac{i}{\hbar}\right)^{3}\mu^{4}e^{-i\omega(t_{1}+t_{3})}e^{-g(t_{1})-g(t_{2})-g(t_{3})+g(t_{1}+t_{2})+g(t_{2}+t_{3})-g(t_{1}+t_{2}+t_{3})}
\end{aligned} \tag{6.35}$$

The line shape function $g(t)$ now is a complex function, and R_1, R_4 and R_2, R_3 are no longer equal. This is since e.g. R_2 is propagating on the electronically excited state during the period t_2, while R_3 is propagating on the electronic ground state, and the excited state H_1 and ground state H_0 Hamiltonians are different.

The correlation function

$$C(t)=\frac{1}{\hbar^{2}}\left\langle \Omega\left(t\right)\Omega\left(0\right)\rho\left(-\infty\right)\right\rangle \tag{6.36}$$

has two important symmetries. The first is:

$$C(-t)=C^{*}(t) \tag{6.37}$$

which we see from:

$$\begin{aligned}
C(-t) &= \left\langle \Omega\left(-t\right)\Omega\left(0\right)\rho\left(-\infty\right)\right\rangle \\
&= \left\langle \Omega\left(0\right)\Omega\left(t\right)\rho\left(-\infty\right)\right\rangle \\
&= \left\langle \rho\left(-\infty\right)\Omega\left(0\right)\Omega\left(t\right)\right\rangle \\
&= \left\langle \Omega\left(t\right)\Omega\left(0\right)\rho\left(-\infty\right)\right\rangle ^{*}
\end{aligned} \tag{6.38}$$

where we have used in the first step the fact that the correlation function depends only on the time interval between the first and the second action of the energy gap

operator on the density matrix, in the second step the invariance of the trace on cyclic permutation, and in the third step the fact that all operators are Hermitian.

We separate the correlation function into its real and imaginary part:

$$\begin{aligned} C(t) &\equiv C'(t) + iC''(t) \\ C'(t) &= \frac{1}{2}\left(C(t) + C^*(t)\right) \\ C''(t) &= \frac{1}{2}\left(C(t) - C^*(t)\right) \end{aligned} \tag{6.39}$$

where C'(t) and C"(t) are both real functions and C'(t) is an even function and C"(t) is an odd function. In frequency domain, we introduce the spectral densities:

$$\begin{aligned} \tilde{C}(\omega) &= \int_{-\infty}^{\infty} dt e^{i\omega t} C(t) = 2Re \int_{0}^{\infty} dt e^{i\omega t} C(t) \\ \tilde{C}'(\omega) &= \int_{-\infty}^{\infty} dt e^{i\omega t} C'(t) = 2 \int_{0}^{\infty} dt \cos(\omega t) C'(t) \\ \tilde{C}''(\omega) &= -i \int_{-\infty}^{\infty} dt e^{i\omega t} C''(t) = 2 \int_{0}^{\infty} dt \sin(\omega t) C''(t) \end{aligned} \tag{6.40}$$

$\tilde{C}(\omega)$, $\tilde{C}'(\omega)$ and $\tilde{C}''(\omega)$ are all real functions, $\tilde{C}'(\omega)$is an even function, and $\tilde{C}''(\omega)$ an odd function. The second symmetry is for $\tilde{C}(\omega)$, which satisfies a detailed balance condition:

$$\tilde{C}(-\omega) = e^{-\frac{\hbar\omega}{k_B T}} \tilde{C}(\omega) \tag{6.41}$$

We see that when expanding Equ. 6.36 in an eigenstate basis of the nuclear coordinates:

$$C(t) = \frac{1}{\hbar^2} \sum_i \sum_{a,b} e^{-\frac{\varepsilon_a^{(i)}}{k_B T}} \left|\Omega_{ab}\right|^2 e^{-i\omega_{ba}^{(i)} t} / Z^{(i)} \tag{6.42}$$

where the first sum runs over all modes coupled to the electronic transition, and the second sum runs over all vibrational states a, b of mode i, and $Z^{(i)} = \sum_a e^{-\frac{\varepsilon_a^{(i)}}{k_B T}}$is the partition function. The Boltzmann factor describes the thermal population of the starting state a. We then obtain for the spectral density:

$$\tilde{C}(\omega) = \frac{1}{\hbar^2} \sum_i \sum_{a,b} e^{-\frac{\varepsilon_a^{(i)}}{k_B T}} \left|\Omega_{ab}\right|^2 \delta(\omega - \omega_{ba}^{(i)}) / Z^{(i)} \tag{6.43}$$

When replacing ω by $-\omega$, the energy levels a and b are interchanged, and we get Equ. 6.41. Combining Equ. 6.40 and 6.41 yields

$$\tilde{C}'(\omega) = \frac{1 + e^{-\frac{\hbar\omega}{k_B T}}}{2}\tilde{C}(\omega) \tag{6.44}$$

and

$$\tilde{C}''(\omega) = \frac{1 - e^{-\frac{\hbar\omega}{k_B T}}}{2}\tilde{C}(\omega) \tag{6.45}$$

Hence, due to the symmetries of Equ. 6.37 and 6.41, the spectral densities $\tilde{C}(\omega)$, $\tilde{C}'(\omega)$ and $\tilde{C}''(\omega)$ are all connected. When we know the imaginary part, we also know the real part and *vice versa*. In other words, even though the line shape function in the Brownian oscillator model is a more complicated function (i.e. it is a complex function), we don't need to have more knowledge about the system than in Kubo lineshape theory. For example, when we would obtain the real part of the frequency fluctuation correlation function from a classical molecular dynamic simulation, we would also know the imaginary part according to Equ. 6.44 and 6.45. The existence of an imaginary part in the frequency fluctuation correlation function is a consequence of the system being quantum mechanical. Nevertheless, we can use the result from a fully classical simulation to predict the properties of the corresponding quantum system.

Finally, let's study the following simple example for the spectral density:

$$\tilde{C}''(\omega) = 2\lambda\frac{\omega/\tau_c}{\omega^2 + 1/\tau_c^2} \tag{6.46}$$

for which we obtain in the high temperature limit $k_B T/\hbar >> 1/\tau_c$:

$$g(t) = \frac{2\lambda k_B T \tau_c^2}{\hbar}\left[e^{-\frac{t}{\tau_c}} + \frac{t}{\tau_c} - 1\right] - i\lambda\tau_c\left[e^{-\frac{t}{\tau_c}} + \frac{t}{\tau_c} - 1\right] \tag{6.47}$$

The real part of this line shape function is the same as the Kubo-line shape function (see Equ. 5.22) with fluctuation amplitude

$$\Delta^2 = 2\lambda k_B T/\hbar \tag{6.48}$$

which depends linearly on temperature. This can be easily seen from the following picture:

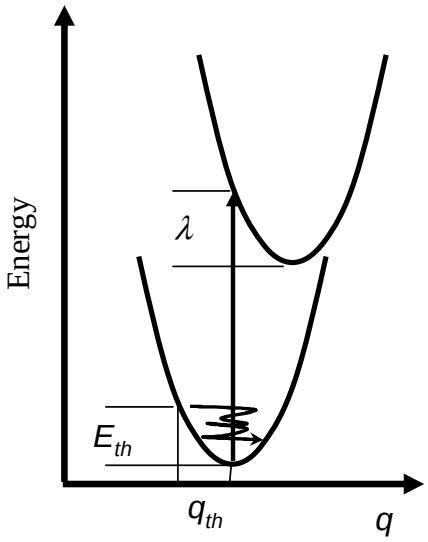

The system will explore regions in the ground state with energy $E_{th} = k_B T$, i.e. the thermal displacement of the nuclear coordinate is given by

$$q_{th}^2 = k_B T/\hbar\omega \tag{6.49}$$

For a system of displaced oscillators, the energy gap will vary linearly with nuclear coordinate with a slope χ. Hence, thermal fluctuations of the nuclear coordinate will give rise to fluctuations of the energy gap with amplitude:

$$\Delta^2 = \chi^2 q_{th}^2 = \chi^2 k_B T/\hbar\omega \tag{6.50}$$

Comparing Equ. 6.48 with Equ. 6.50, we see that the parameter λ resembles the reorganization energy (or the Stokes shift, see below):

$$\lambda = \chi^2\omega \tag{6.51}$$

Hence, we have described the fluctuation amplitude Δ, which in the Kubo model is just a phenomenological parameter, by two measurable quantities, namely the temperature and the displacement of the excited state potential. Note that the imaginary part of the line shape function is independent on temperature. When we separate the line shape function into real and imaginary part:

$$g(t) = g'(t) - ig''(t) \tag{6.52}$$

and insert this into the definition of the absorption spectrum:

$$A(\omega) = 2\mu^2\Re\int_0^\infty dt e^{i\omega-\omega_0 t}e^{-g(t)} = 2\mu^2\Re\int_0^\infty dt e^{i(\omega-\omega_0 t-g''(t))}e^{-g'(t)} \tag{6.53}$$

we see that the imaginary part corresponds to a frequency shift. If we would calculate the corresponding expression for the fluorescence spectrum, we would find that the shift is in the opposite direction. This gives rise to the *Stokes shift*, which in general is time dependent:

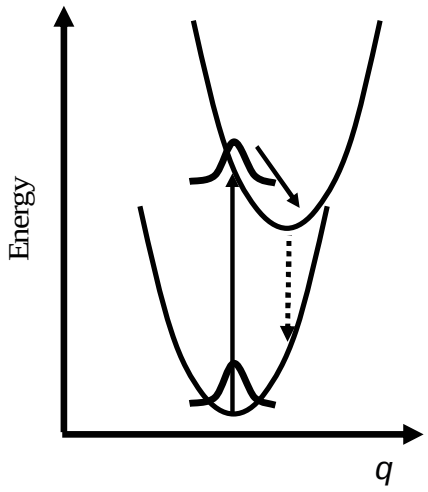

In a dynamic Stokes shift experiment, a pump pulse projects the thermal ground state distribution onto the excited state potential surface. The system then will be in a non-equilibrium situation, and it will start to relax towards the bottom of the excited state potential surface. We can follow this relaxation by monitoring the fluorescence spectrum as a function of time, for which we will observe a transient red-shift described by the imaginary part $g"(t)$ of the line shape function.

The size of the Stokes shift λ measured relative to the width of the absorption spectrum Δ (i.e. the width of the frequency fluctuations in the slow modulation limit) is:

$$\frac{\lambda}{\Delta} = \frac{\hbar\Delta}{2k_BT} \tag{6.54}$$

Hence, we see that whenever the width of an absorption line is comparable to k_BT or larger, we have to take into account the effect of the Stokes shift and have to use the complex line shape function Equ. 6.34. This is in general the case for electronic transitions. However, when $\Delta << k_BT$, the significance of the Stokes shift disappears, and the stochastic ansatz Equ. 5.20 describes the problem sufficiently well. This is in general the case for vibrational transitions and in particular for spin transitions. Kubo lineshape theory has initially been developed for the latter

7 2D Spectroscopy: Measuring the 3^{rd}-Order Response Function Directly

7.1 2D Spectroscopy of a Single Transition

In it's most general form, a 2D experiment uses the geometry of a 3-pulse photon echo setup, with the difference that the 3^{rd}-order polarization is measured by heterodyning it with a 4^{th} replica of the laser pulses (the so-called local oscillator), rather than by homodyne-detecting it directly (as done in Sec. 5.3).

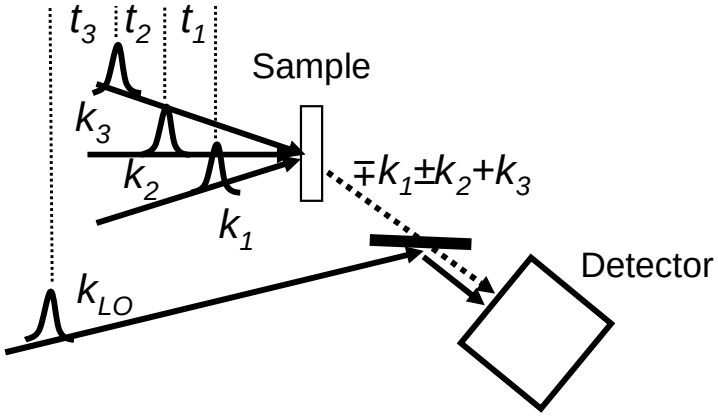

Rephasing diagrams are collected in the $-k_1 + k_2 + k_3$-direction, while non-rephasing diagrams are collected in the $+k_1 - k_2 + k_3$-direction. For the case of a two-level system, the corresponding Feynman diagrams are :

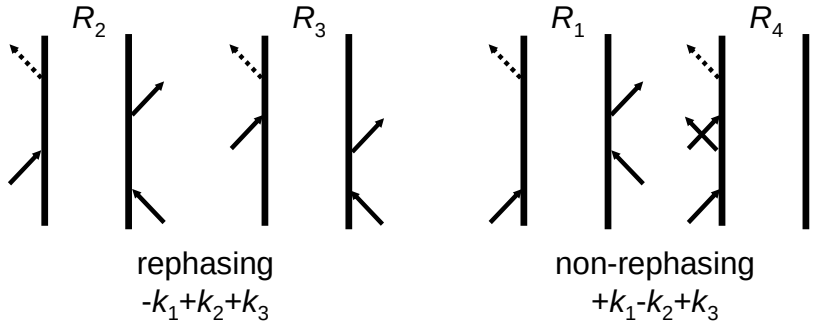

and the corresponding response functions are for the rephasing diagrams (in the most simple picture of purely phenomenological dephasing):

$$R_2 = R_3 \propto e^{+i\omega t_1} e^{-\Gamma t_1} e^{-i\omega t_3} e^{-\Gamma t_3} \tag{7.1}$$

and for the non-rephasing diagrams:

$$R_1 = R_4 \propto e^{-i\omega t_1} e^{-\Gamma t_1} e^{-i\omega t_3} e^{-\Gamma t_3} \tag{7.2}$$

with

$$\omega = (\epsilon_1 - \epsilon_0)/\hbar \tag{7.3}$$

As a result of the interference between the emitted light and the local oscillator, one is measuring the electric field:

$$\int_0^\infty \left| E_0(t) + iP^{(3)}(t) \right|^2 dt \approx \int_0^\infty |E_0(t)|^2 + 2\Im\left(E_0(t)P^{(3)}(t)\right) dt \tag{7.4}$$

rather than its intensity:

$$\int_0^\infty \left| P^{(3)}(t) \right|^2 dt \tag{7.5}$$

In contrast to the photon echo experiment, the heterodyned signal is no longer background free, but sits on an offset $\int_0^\infty |E_0(t)|^2 dt$ (which normally is subtracted).

Ideally, one uses δ-shaped pulses for the three input pulses as well as for the local oscillator. In this case, one obtains as the measurement signal the response function itself:

$$\int_0^\infty \Im\left(E_0(t)P^{(3)}(t)\right) dt \propto S^{(3)}(t_3, t_2, t_1) \tag{7.6}$$

without any complication due to a convolution etc. Times t_1, t_2, and t_3 are the delay times directly controlled by the experiment. In that sense, 2D spectroscopy is the ultimate nonlinear experiment, since it gathers the maximum amount of information (within the framework of 3^{rd}-order spectroscopy). What we cannot learn with 2D spectroscopy, we will not be able to learn with any other 3^{rd}-order spectroscopy. The prize we pay for this completeness, however, is: $S^{(3)}(t_3, t_2, t_1)$ is a three-dimensional oscillating function which is very complex and almost impossible to visualize. This is why heterodyne-detected photon echoes, initially pioneered by Wiersma already in the mid-90's, were not considered to be anything useful for quite some time.

The simple trick to visualize such a function is to transform it into frequency space by the help of a 2D Fourier transformation (it took quite some time to realize that):

$$S^{(3)}(\omega_3, t_2, \omega_1) = \int_0^\infty \int_0^\infty S^{(3)}(t_3, t_2, t_1) e^{+i\omega_3 t_3} e^{\mp i\omega_1 t_1} dt_1 dt_3 \tag{7.7}$$

where the '$\mp$' is for rephasing and non-repahsing diagrams, respectively (see below). The Fourier transform is performed with respect to the coherence times t_1 and t_3, while time t_2, where the system is in a population state (also called waiting time), is not transformed. This leads to 2D spectra, which are much more intuitive than the signal in the time-domain $S^{(3)}(t_3, t_2, t_1)$. A sequence of 2D spectra for various waiting times t_2 gives the full information about the 3^{rd}-order response function $S^{(3)}(\omega_3, t_2, \omega_1)$.

The Fourier transforms of Eq. 7.9 and Eq. 7.2:

$$R_{2,3}(\omega_1, \omega_3) \propto \frac{1}{-i(\omega_1 - \omega) - \Gamma} \cdot \frac{1}{+i(\omega_3 - \omega) - \Gamma} \tag{7.8}$$
$$R_{1,4}(\omega_1, \omega_3) \propto \frac{1}{+i(\omega_1 - \omega) - \Gamma} \cdot \frac{1}{+i(\omega_3 - \omega) - \Gamma}$$

are complex-valued, and one may either plot the real, the imaginary or the absolute value of the outcome. However, it turns out that neither of it are very intuitive. They contain both absorptive and dispersive contributions, which makes the band (a) broad, and/or which (b) renders the band positive and negative in certain regions:

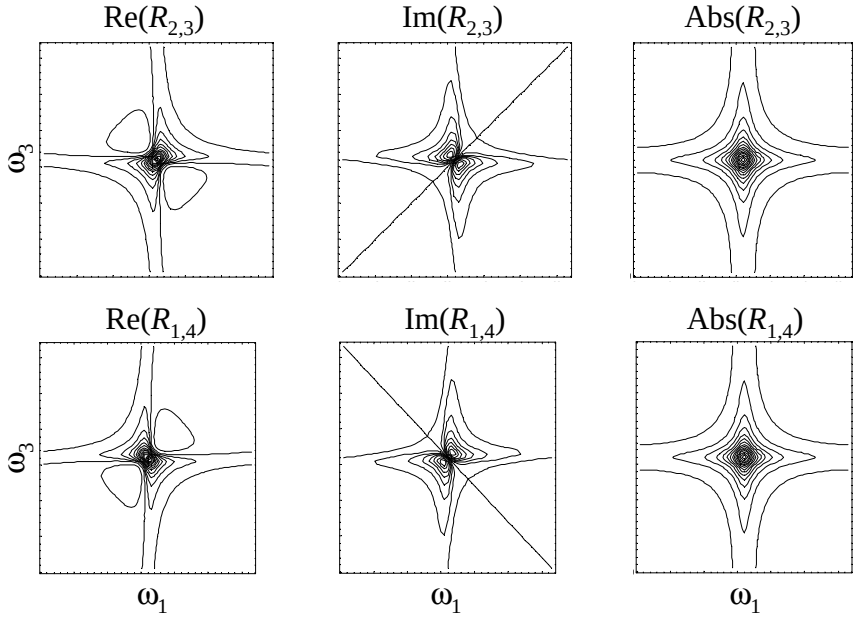

It is now established that it is the best to plot the real part of the sum of both spectra:

$$R_{abs}(\omega_1, \omega_3) = \Re\left(R_{2,3}(\omega_1, \omega_3) + R_{1,4}(\omega_1, \omega_3)\right) \tag{7.9}$$

which yields so-called purely absorptive spectra:

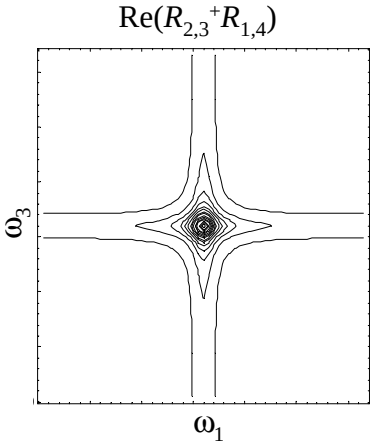

The purely absorptive spectrum yields the sharpest lines and it preserves the sign of the response function (in contrast to the absolute-valued spectrum shown above). The latter will be important when we deal with more than one transition. The prize we pay is: We need to collect two sets of data under exactly identical conditions, and, we need to know the absolute phase of both of these signals (in contrast to the absolute-valued spectrum, which is the easiest to measure).

7.2 2D Spectroscopy in the Presence of Spectral Diffusion

under construction

7.3 2D Spectroscopy of a Set of Coupled Oscillators

Consider a level scheme of two coupled vibrational oscillators:

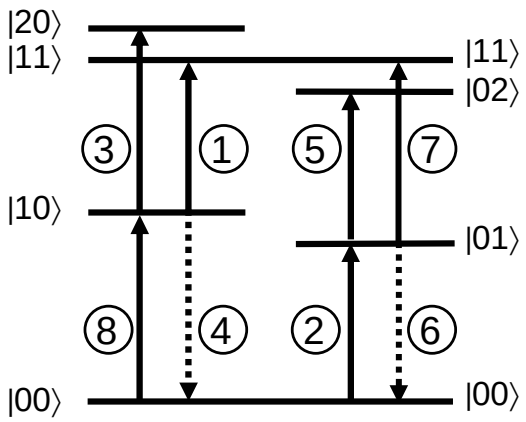

where $|ij\rangle$ denotes a state with i quanta in the first oscillator #1 and j quanta in the second oscillator #2. From the ground state we can either excite state $|10\rangle$ or state $|10\rangle$. From either of these states, we have three possibilities. When we start for example from $|10\rangle$, then we have $|10\rangle \rightarrow |00\rangle$ (stimulated emission), $|10\rangle \rightarrow |20\rangle$ (up-climbing of oscillator #1), or $|10\rangle \rightarrow |11\rangle$. The transition $|10\rangle \rightarrow |02\rangle$ is forbidden (in the harmonic approximation) since it would require a 3-quanta transition.

The set of Feynman diagrams we have to consider is for the $k_1 - k_2 + k_3$-direction:

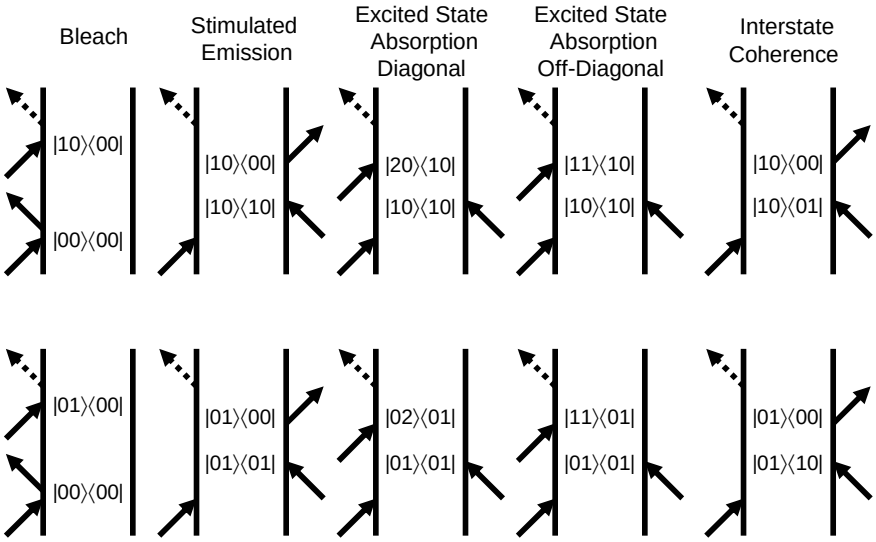

A corresponding set of Feynman diagrams exists for the $-k_1 + k_2 + k_3$-direction. The 'interstate-coherence' diagrams play special role, as they oscillate as a function of population time t_2. In most cases, one will measure with $t_2 = 0$, in which case the 'interstate-coherence' diagrams result in the same signal as the bleach and stimulated emission diagrams.

The following picture shows an example of a purely absorptive 2D-IR spectrum of the two C=O vibrations of dicabonylacetyl-acetonato rhodium (I) (RDC) (kindly provided by Andrei Tokmakoff, see Phys. Rev. Lett. 90, 047401 (2003)):

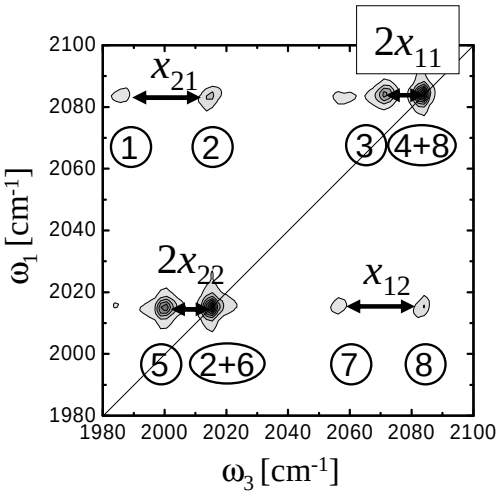

Each peak is such a spectrum corresponds to one of the possible transitions (labelled by numbers), and the 2D-lineshape of each peak is that described in Sec. 7.1 or Sec. 7.2, respectively.

We find so-called diagonal contributions in the 2D spectrum (peaks 5, (2+6), 3 and (4+8)) and off-diagonal contributions (peaks 1, 2, 7, and 8). Each diagonal and off-diagonal peaks consist of a pair of peaks with positive and negative amplitudes (indicated as blue and red, respectively). For example, the blue diagonal peak labelled with 6 corresponds to the $|01\rangle \rightarrow |00\rangle$ stimulated emission, while the red diagonal peak labelled with 5 corresponds to the $|01\rangle \rightarrow |02\rangle$ excited state absorption. Diagonal peaks involve one oscillator only. Since the oscillator is slightly anharmonic, the $|01\rangle \rightarrow |02\rangle$ excited state absorption is red-shifted with respect to the $|01\rangle \rightarrow |00\rangle$ stimulated emission. If the oscillator were harmonic, both signals would overlap and cancel completely.

As an example of an off-diagonal peak, the signal labelled 2 corresponds to the bleach of the $|01\rangle$ oscillator, while the signal labelled 1 corresponds to the $|10\rangle \rightarrow |11\rangle$ absorption. In both cases, we observe the excitation frequency of the second oscillator, with the difference that in the one case (1) the first oscillator is excited as well, while it is not in the second case (2). If both oscillator would not see each other, the second oscillator would not care about the excitation of the first. Then, both signals (1) and (2) would again coincide and the off-diagonal contribution would disappear. In that sense, the existence of a cross peak tells something about the coupling between vibrational modes.

7.4 The Exciton Model for Weakly Coupled Vibrational States

In order to calculate diagonal and off-diagonal contribution of a 2D-IR spectrum, one needs to calculate the so-called diagonal (x_{ii}) and off-diagonal ($x_{ij}, i \neq j$) anharmonicities, which are the constants of a Dunham expansion:

$$E = \sum_i \epsilon_i (n_i + \frac{1}{2}) - \sum_{i \leq j} x_{ij} (n_i + \frac{1}{2})(n_j + \frac{1}{2}) + \dots \tag{7.10}$$

The splittings of the diagonal and off-diagonal peaks in the 2D-spectrum relate directly to these constants. However, in order to calculate them, one would need to calculate cubic and quartic force constants of the molecules potential energy surface, which is a difficult task. As an alternative, there is a simplified model, the so-called exciton model, which is often used and which describes the 2D-IR spectroscopy of weakly coupled vibrational states reasonably well.

Coupled *Harmonic* Oscillators: A system of coupled harmonic oscillators is described by the Hamiltonian:

$$H = \sum_i \epsilon_i b_i^\dagger b_i + \sum_{i<j} \beta_{ij} (b_i^\dagger b_j + b_j^\dagger b_i). \tag{7.11}$$

Here, $b_i^\dagger$ and b_i are the creation and annihilation operators of individual oscillators, respectively. The ϵ_i are the intrinsic excitation energies of the individual sites, and the β_{ij} are the couplings between sites. The Hamiltonian conserves the number of excitations and hence separates into blocks of the ground-state, the one-excitonic Hamiltonian $H_1^{(0)}$, the two-excitonic Hamiltonian $H_2^{(0)}$, etc. When expanding the Hamiltonian in a site basis

$$\{|0,0\rangle, |1,0\rangle, |0,1\rangle, |2,0\rangle, |0,2\rangle, |1,1\rangle\}, \tag{7.12}$$

(using the same convention as above) the harmonic Hamiltonian reads

$$H^{(0)} = \left(\begin{array}{c|cc|ccc} 0 & & & & & \\ \hline & \epsilon_1 & \beta_{12} & & & \\ & \beta_{12} & \epsilon_2 & & & \\ \hline & & & 2\epsilon_1 & 0 & \sqrt{2}\beta_{12} \\ & & & 0 & 2\epsilon_2 & \sqrt{2}\beta_{12} \\ & & & \sqrt{2}\beta_{12} & \sqrt{2}\beta_{12} & \epsilon_1 + \epsilon_2 \end{array}\right) \tag{7.13}$$

Here, the zero-, one-, and two-exciton manifolds have been separated by lines. In the harmonic case, we know without explicit diagonalization of the harmonic two-excitonic Hamiltonian that its eigenstates (i.e. the two-excitonic states) are product states of the one-excitonic states (harmonic oscillators decouple). In that sense, the one-exciton Hamiltonian:

$$H_1^{(0)} = \begin{pmatrix} \epsilon_1 & \beta_{12} \\ \beta_{12} & \epsilon_2 \end{pmatrix} \tag{7.14}$$

already contains all the physics of a harmonic system.

Coupled *Anharmonic* Oscillators: However, as a very general argument one can state that the nonlinear response of a harmonic system vanishes; any nonlinear experiment would reveal a zero-signal. Diagonalization of the Hamiltonian would reveal $x_{ij} = 0$ for all anharmonic constants, and each pair of peaks on the diagonal and on the off-diagonal of the 2D spectrum would just coincide and cancel each other. Hence, we have to include anharmonicity in order to understand the nonlinear spectroscopic response of a system of coupled oscillators. Anharmonicity is generally included in an *ad hoc* manner by lowering the site energies of the doubly-excited site-states by an energy Δ:

$$H = \left(\begin{array}{c|cc|ccc} 0 & & & & & \\ \hline & \epsilon_1 & \beta_{12} & & & \\ & \beta_{12} & \epsilon_2 & & & \\ \hline & & & 2\epsilon_1 - \Delta & 0 & \sqrt{2}\beta_{12} \\ & & & 0 & 2\epsilon_2 - \Delta & \sqrt{2}\beta_{12} \\ & & & \sqrt{2}\beta_{12} & \sqrt{2}\beta_{12} & \epsilon_1 + \epsilon_2 \end{array}\right) \tag{7.15}$$

The magnitude of the site-anharmonicity Δ can be determined from pump-probe experiments of a single uncoupled vibrator. In the weak-coupling limit $\beta_{12} \ll |\epsilon_2 - \epsilon_1|$, the two-excitonic states can still be identified as product states of the one-excitonic states, lowered in energy by diagonal and off-diagonal anharmonicity. The latter can be calculated perturbatively:

$$x_{12} = 4\Delta \frac{\beta_{12}^2}{(\epsilon_2 - \epsilon_1)^2} \tag{7.16}$$

so that the off-diagonal anharmonicity reflects directly the anharmonic coupling.

The exciton model has been used extensively to describe 2D-IR spectra of the so-called amide I band of small peptides. In this case, the C=O groups of the peptide backbone are thought to be coupled mostly through electrostatic interaction, which in the most simple approximation can be described as dipol-dipol-coupling:

$$\beta_{ij} = \frac{1}{4\pi\epsilon_0}\left[\frac{\vec{\mu}_i \cdot \vec{\mu}_j}{r_{ij}^3} - 3\frac{(\vec{r}_{ij} \cdot \vec{\mu}_i)(\vec{r}_{ij} \cdot \vec{\mu}_j)}{r_{ij}^5}\right] \tag{7.17}$$

The strength of this coupling is given by distance and relative orientation of the C=O groups, and hence is directly related to the geometry of the molecule. A review on this topic can be found in [Woutersen and Hamm, J. Phys.: Condens. Matter 14 (2002) R1035]

Final Remark: There are many variants of experimental realizations of 2D spectroscopy. The most important variant is obtained by introducing a spectrometer in front of the detector:

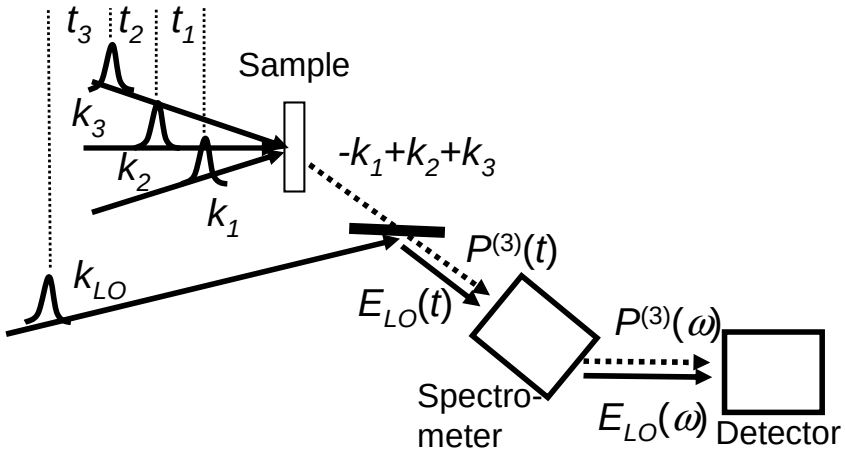

The action of this spectrometer is to perform the Fourier-transform with respect to t_3. Scanning of t_3 is no longer needed. When using an array detector that covers the whole ω_3-frequency range of interest in one shot, this actually reduces the measurement time significantly since only one time axis t_1 needs to be scanned.

The second variant of 2D spectroscopy is the so-called double-resonance experiment, which shall not be discussed any further here. The relation between the double-resonance experiment and the heterdyne detected photon echo experiment has been analyzed in depth in [JCP 121 (2004) 5935-5942].